Cellulose Nanocrystals: Chemistry, Self-Assembly, and Applications

Youssef Habibi,[†] Lucian A. Lucia,*[,†] and Orlando J. Rojas[†,‡]

Department of Forest Biomaterials, North Carolina State University, Box 8005, Raleigh, North Carolina 27695-8005, and Department of Forest Products Technology, Faculty of Chemistry and Materials Sciences, Helsinki University of Technology, P.O. Box 3320, FIN-02015 TKK, Espoo, Finland

Received October 12, 2009

Contents

1. Introduction and State of the Art

Cellulose constitutes the most abundant renewable polymer resource available today. As a chemical raw material, it is generally well-known that it has been used in the form of fibers or derivatives for nearly 150 years for a wide spectrum of products and materials in daily life. What has not been known until relatively recently is that when cellulose fibers are subjected to acid hydrolysis, the fibers yield defect-free, rod-like crystalline residues. Cellulose nanocrystals (CNs) have garnered in the materials community a tremendous level of attention that does not appear to be relenting. These biopolymeric assemblies warrant such attention not only because of their unsurpassed quintessential physical and chemical properties (as will become evident in the review) but also because of their inherent renewability and sustainability in addition to their abundance. They have been the subject of a wide array of research efforts as reinforcing agents in nanocomposites due to their low cost, availability, renewability, light weight, nanoscale dimension, and unique morphology. Indeed, CNs are the fundamental constitutive polymeric motifs of macroscopic cellulosic-based fibers whose sheer volume dwarfs any known natural or synthetic biomaterial. Biopolymers such as cellulose and lignin and

Dr. Youssef Habibi is a research assistant professor at the Department of Forest Biomaterials at North Carolina State University. He received his Ph.D. in 2004 in organic chemistry from Joseph Fourier University (Grenoble, France) jointly with CERMAV (*Centre de Recherche sur les Macromolécules Végétales*) and Cadi Ayyad University (Marrakesh, Morocco). During his Ph.D., he worked on the structural characterization of cell wall polysaccharides and also performed surface chemical modification, mainly TEMPO-mediated oxidation, of crystalline polysaccharides, as well as their nanocrystals. Prior to joining NCSU, he worked as assistant professor at the French Engineering School of Paper, Printing and Biomaterials (PAGORA, Grenoble Institute of Technology, France) on the development of biodegradable nanocomposites based on nanocrystalline polysaccharides. He also spent two years as postdoctoral fellow at the French Institute for Agricultural Research, INRA, where he developed new nanostructured thin films based on cellulose nanowiskers. Dr. Habibi's research interests include the sustainable production of materials from biomass, development of high performance nanocomposites from lignocellulosic materials, biomass conversion technologies, and the application of novel analytical tools in biomass research.

[†] North Carolina State University.
[‡] Helsinki University of Technology.

10.1021/cr900339w
Published on Web 03/04/2010

Dr. Lucian A. Lucia is currently an associate professor who works in the area of renewable materials chemistry and engineering in the Department of Forest Biomaterials (formerly Wood & Paper Science) at North Carolina State University. He received his Ph.D. in 1996 under Prof. Kirk S. Schanze from the University of Florida (Gainesville, FL) in organic chemistry with a focus on modeling the fundamental electron transfer pathways active in plant photosynthesis. He then spent almost 2 years at the NSF Center for Photoinduced Charge Transfer at the University of Rochester (Rochester, NY, under Prof. David G. Whitten) where he explored the design of highly functional materials based on photoactive amphiphiles and their behavior in heterogeneous media. He began his independent academic career as an assistant professor at the Institute of Paper Science and Technology at the Georgia Institute of Technology (Atlanta, GA) in 1997 where he extensively studied the materials chemistry and photochemistry of wood biopolymers. He joined the faculty at North Carolina State University in 2004 where he began to explore fundamental and applied aspects of renewable material-based composites. His research interests include antibacterial materials, cellulose nanocrystal templates, scaffolds for tissue engineering, drug delivery devices, biomass pretreatments, and wood pulping chemistry.

Dr. Orlando Rojas is Associate Professor in North Carolina State University and Finland Distinguished Professor in Helsinki University of Technology. He worked as a Senior Scientist in the Department of Chemistry, Physical Chemistry of the Royal Institute of Technology, KTH, and in the Institute for Surface Chemistry, YKI. Prior appointments include his tenure as professor in the Department of Chemical Engineering of Universidad de Los Andes (Venezuela), after obtaining his Ph.D. in Chemical Engineering in Auburn University and other graduate degrees that included a Diploma in Paper Engineering from the ETSII of Universidad Politecnica de Cataluña (Spain). He leads the "Colloids and Interfaces" Group at NC State University with a research focus on surface and colloid chemistry and the adsorption behaviors of surfactants and polymers at solid/liquid interfaces. He has studied the viscoelasticity of adsorbed monolayers by surface laser light scattering, surface plasmon resonance, and quartz crystal microgravimetry methods. His work has also involved state-of-the-art interferometric and bimorph surface force techniques, as well as atomic force microscopy, to unveil basic phenomena and interactions at the nanoscale. His group currently works on nanocellulose structures, the dynamics of lignocellulose degradation, biosensor development, and separation, derivatization, and use of natural polymers and surfactants. He is Associate Editor of the *Journal of Surfactants and Detergents* and member of the advisory committee of several other journals. Dr. Rojas is the 2009−2010 Chair of the Division of "Cellulose and Renewable Materials" of the American Chemical Society and is the recipient of the 2009 American Chemical Society Divisional service Award. He was appointed 2009−2014 Finland Distinguish Professor by Tekes, the Finnish Funding Agency for Technology and Innovation and the Academy of Finland.

in some cases heteropolysaccharides provide the hierarchical constructs to bioengineer biological factories that give rise to a variegated distribution of plants and organisms. Surprisingly, a focus on nanoscale phenomena involving these materials has not been realized until the past few years in which a virtual collection of information has become available.

In the following review, the salient chemical and physical features of the most dominant fundamental building block in the biosphere, cellulose nanocrystals, are discussed. After a brief introduction to cellulose, three general aspects of CNs are covered, namely, their morphology and chemistry including their preparation and chemical routes for functionalization, self-assembly in different media and under different conditions, and finally their applications in the nanocomposites field. While these aspects are by no means comprehensively inclusive of the vast number of research results available, they may be regarded as perhaps the most scientifically and technologically pertinent aspects of CNs that deserve attention.

2. Structure and Morphology of Celluloses

Cellulose is the most abundant renewable organic material produced in the biosphere, having an annual production that is estimated to be over 7.5×10^{10} tons.[1] Cellulose is widely distributed in higher plants, in several marine animals (for example, tunicates), and to a lesser degree in algae, fungi, bacteria, invertebrates, and even amoeba (protozoa), for example, *Dictyostelium discoideum*. In general, cellulose is a fibrous, tough, water-insoluble substance that plays an essential role in maintaining the structure of plant cell walls. It was first discovered and isolated by Anselme Payen in 1838,[2] and since then, multiple physical and chemical aspects of cellulose have been extensively studied; indeed, discoveries are constantly being made with respect to its biosynthesis, assembly, and structural features that have inspired a number of research efforts among a broad number of disciplines. Several reviews have already been published reporting the state of knowledge of this fascinating polymer.[1,3−13]

Regardless of its source, cellulose can be characterized as a high molecular weight homopolymer of β-1,4-linked anhydro-D-glucose units in which every unit is corkscrewed 180° with respect to its neighbors, and the repeat segment is frequently taken to be a dimer of glucose, known as cellobiose (Figure 1). Each cellulose chain possesses a directional chemical asymmetry with respect to the termini of its molecular axis: one end is a chemically reducing functionality (i.e., a hemiacetal unit) and the other has a pendant hydroxyl group, the nominal nonreducing end. The number of glucose units or the degree of polymerization (DP) is up to 20 000, but shorter cellulose chains can occur and are mainly localized in the primary cell walls.

All β-D-glucopyranose rings adopt a $^4C_1$ chair conformation, and as a consequence, the hydroxyl groups are positioned in the ring (equatorial) plane, while the hydrogen atoms are in the vertical position (axial). This structure is

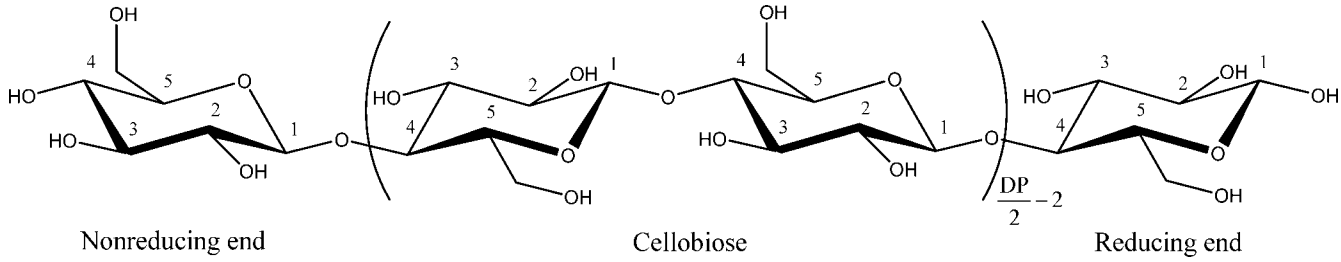

Figure 1. Chemical structure of cellulose.

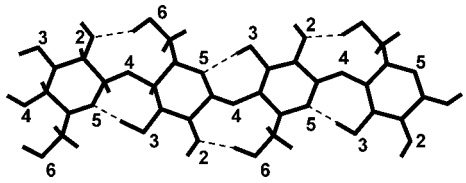

Figure 2. Intramolecular hydrogen-bonding network in a representative cellulose structure.

stabilized by an intramolecular hydrogen bond network extending from the O(3′)-H hydroxyl to the O(5) ring oxygen of the next unit across the glycosidic linkage and from the O(2)-H hydroxyl to the O(6′) hydroxyl of the next residue (Figure 2).

The three most probable rotational positions of the hydroxymethyl group are defined by ascertaining the placement of the O6−C6 bond with respect to the O5−C5 and C4−C5 bonds: if O6−C6 is *gauche* to O5−C5 and *trans* to C4−C5, then the conformation is called *gt*, while the other two conformations are referred to as *gg* and *tg* (Figure 3).

In nature, cellulose does not occur as an isolated individual molecule, but it is found as assemblies of individual cellulose chain-forming fibers. This is because cellulose is synthesized as individual molecules, which undergo spinning in a hierarchical order at the site of biosynthesis. Typically, approximately 36 individual cellulose molecules assemble are brought together into larger units known as elementary fibrils (protofibrils), which pack into larger units called microfibrils, and these are in turn assembled into the familiar cellulose fibers. However, celluloses from different sources may occur in different packing as dictated by the biosynthesis conditions. The combined actions of biopolymerization, spinning, and crystallization occur in a rosette-shaped plasma membrane complex having a diameter of 30 nm (Figure 4) and are orchestrated by specific enzymatic *terminal complexes* (TCs) that act as biological spinnerets.[14] Because all the cellulose chains in one microfibril must be elongated by the complex at the same rate, crystallization during cellulose synthesis follows very closely polymerization of the chains by the TCs.[15,16] TCs are thought to be cellulose synthase complexes that belong to the large GT-A family of glycosyltransferases; however, the reaction mechanism involved in cellulose synthesis and assembly is still conjectural. The

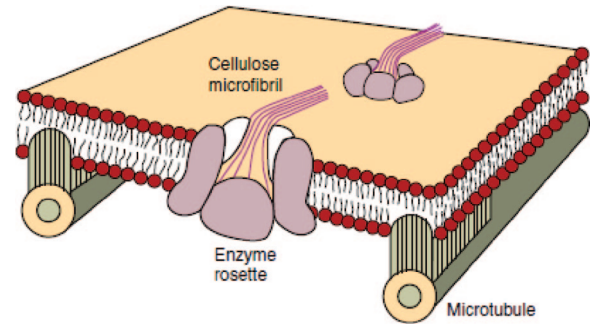

Figure 4. Orientation of microtubules controlling the orientation of cellulose in the cell wall where the microtubules act like tracks to guide the cellulose enzymes floating in the cell membrane. Reprinted with permission from Ref 17. Copyright 2002 Elsevier.

structure of cellulose microfibrils implies that their syntheses and assembly involve the coordinate activity of approximately 36 active sites.[17] However, diverse cellulose structures in various organisms imply that the enzyme complex is modular.[14,18] Recent evidence from live-cell imaging of cellulose indicates that microtubules exert a direct effect on the orientation of cellulose deposition under specific conditions, but microtubules are not required for oriented deposition of cellulose under other conditions (Figure 4).

During the biosynthesis, cellulose chains are aggregated in microfibrils that display cross dimensions ranging from 2 to 20 nm, depending on the source of celluloses. The aggregation phenomenon occurs primarily via van der Waals forces and both intra- (Figure 2) and inter-molecular hydrogen bonds. If the TCs are not perturbed, they can generate a limitless supply of microfibrils having only a limited number of defects or amorphous domains.[14,18] A number of models for the microfibril hierarchy have been proposed that attempt to describe the supramolecular structure of cellulose, including the crystalline structure, crystallite dimensions and defects, structural indices of amorphous domains, dimensions of fibrillar formation, etc. These models differ mainly in the description of the organization and the distribution of the amorphous or less ordered regions within the microfibril. After many years of controversy, it is common practice to acknowledge that the amorphous regions are distributed as chain dislocations on segments along the

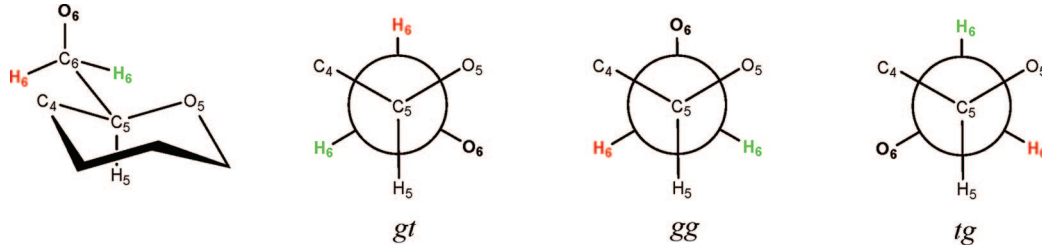

Figure 3. The three most probable rotational positions of the hydroxymethyl group.

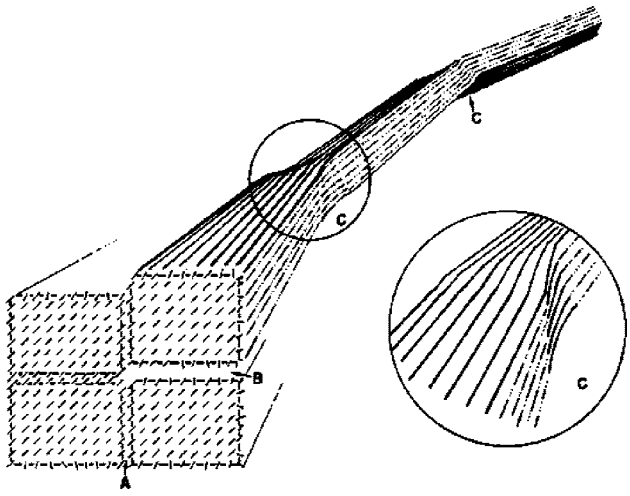

Figure 5. Schematic representation of the elementary fibril illustrating the microstructure of the elementary fibril and strain-distorted regions (defects). Reprinted with permission from Ref 19. Copyright 1972 John Wiley and Sons.

elementary fibril where the microfibrils are distorted by internal strain in the fiber and proceed to tilt and twist (Figure 5).[19]

In the ordered regions, cellulose chains are tightly packed together in crystallites, which are stabilized by a strong and very complex intra- and intermolecular hydrogen-bond network. The hydrogen-bonding network and molecular orientation in cellulose can vary widely, which can give rise to cellulose polymorphs or allomorphs, depending on the respective source, method of extraction, or treament.[1,20] Six interconvertible polymorphs of cellulose, namely, I, II, III_I, III_{II}, IV_I, and IV_{II}, have been identified.

Native cellulose has been thought to have one crystal structure, cellulose I, but evidence for the existence of two suballomorphs of cellulose I, termed Iα and Iβ, was established in 1984 by cross-polarization magic angle spinning (CP-MAS).[21,22] Depending on the origin of cellulose, these two polymorphs exist in different ratios: Iα is prevalent in celluloses from algae and bacteria, and both Iα and Iβ may be present in celluloses in higher plants. However, the latter result is not without controversy. Solid-state NMR studies reported by Atalla and VanderHart[23] has demonstrated several anomalies within the spectra of higher plant celluloses compared with those from algae, bacteria, and tunicates. The anomalies found in the NMR spectra seem to suggest that higher plants may contain only cellulose Iβ, instead of cellulose Iα, with a distorted form of Iβ that resides below the surface.

In both the Iβ and Iα structures, cellulose chains adopt parallel configurations, but they differ in their hydrogen-bonding patterns, which implies a difference in the crystalline structure (Figure 6). Indeed, Iα corresponds to a triclinic $P1$ unit cell (a = 6.717 Å, b = 5.962 Å, c = 10.400 Å, α = 118.08°, β = 114.80°, and γ = 80.37°) containing only one chain per unit cell,[24] whereas Iβ exists in a monoclinic $P2_1$ unit cell having two cellulose chains (a = 7.784 Å, b = 8.201 Å, c = 10.38 Å, α = β = 90°, and γ = 96.5°).[25] Iα, a metastable phase, can be converted to the more thermodynamically stable Iβ phase by high-temperature annealing in various media.[26] Cellulose I (α and β) has sheets stacked in a "parallel-up" fashion, and the hydroxylmethyl groups are oriented in a *tg* conformation so that their O6 atom points toward the O2 hydroxyl groups of the neighboring residue, which engenders a second inter-residue hydrogen bond.[27] If cellulose is bent in a plane orthogonal to the hydrogen-bonded sheets of chains, a horizontal displacement of the sheets with respect to one another is induced.[28] A bending angle of 39° has been shown to be sufficient to induce Iα and Iβ interconversion especially when the curvature of the chain sheets in the microfibril is modeled as a group of concentric circular arcs. *Sine qua non*, all microfibrils

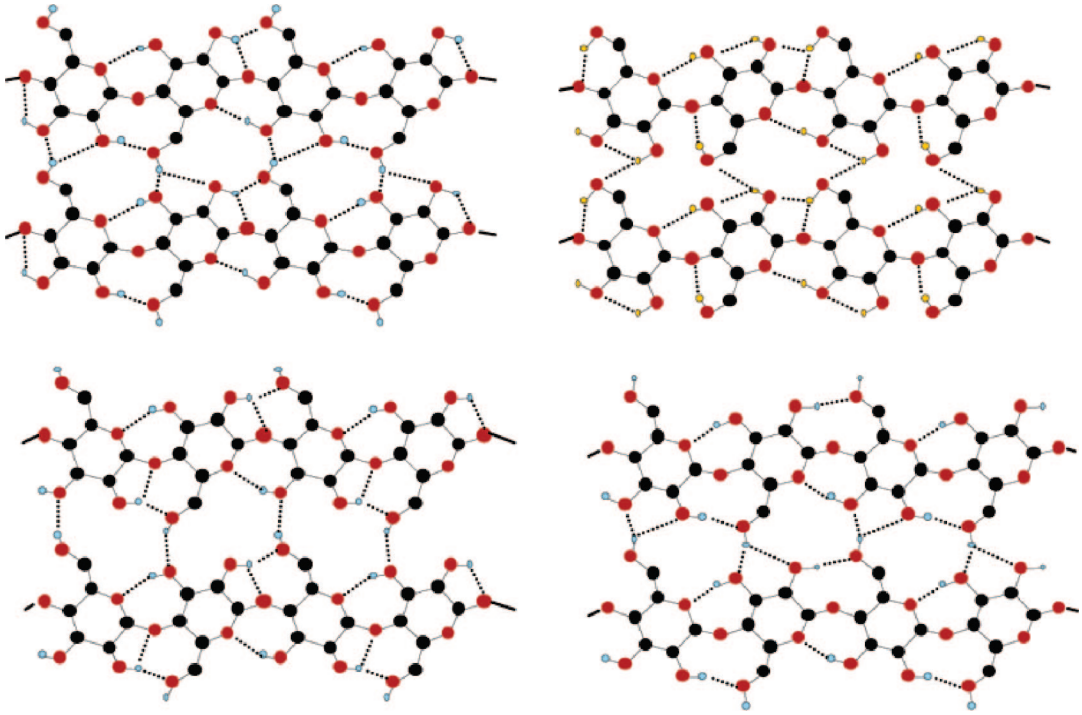

Figure 6. Hydrogen-bonding patterns in cellulose Iα and Iβ: (top) the two alternative hydrogen-bond networks in cellulose Iα; (bottom) the dominant hydrogen-bond network in cellulose Iβ (left) chains at the origin of the unit cell and (right) chains at the center of the unit cell according to Sturcova et al.[32] Reprinted with permission from ref 32. Copyright 2004 American Chemical Society.

generated from the TCs must torque sharply before they can adopt a parallel configuration with respect to the face of the inner cell wall. Therefore, the crystal form is likely to be drastically changed before cellulose is incorporated into the cell wall. Such polymorphic differences were first evidenced by IR spectroscopy[29] and electron diffraction[30] and have been further confirmed more recently by solid-state CP/MAS ^{13}C NMR.[21] The crystal structure and hydrogen-bonding pattern of cellulose I (α and β) were later studied more deeply by synchrotron X-ray and neutron fiber diffraction,[24,25,31] where in the latter, the hydrogen atom positions involved in hydrogen bonding were determined from Fourier-difference analysis with respect to hydrogenated and deuterated samples. The definition of all atomic spatial coordinates in the cellulose crystal structure was only possible for the first time because of the availability of these singular methods.

Cellulose II, the second most extensively studied allomorph, can be obtained by two different processes:

(i) By chemical regeneration, which consists of dissolving cellulose I in a solvent, then reprecipitating it in water. Suitable solvents for cellulose include, among others, solutions of heavy metal−amine complexes, mainly copper with ammonia or diamine such as cupric hydroxide in aqueous ammonia (Scheweizer's reagent called *cuoxam*)[33] or cupriethylenediamine (*cuen*),[34] ammonia or amine/thiocyanate,[35] hydrazine/thiocyanate,[36] lithium chloride/*N*,*N*-dimethylacetamide (LiCl/DMAc),[37,38] and *N*-methylmorpholine-*N*-oxide (NMMO)/water[39−41] systems.

(ii) By mercerization, a universally recognized process the name of which is derived from its inventor John Mercer (1844),[42] which consists of swelling native cellulose in concentrated sodium hydroxide solutions and yielding cellulose II after removing the swelling agent. Other swelling agents, such as nitric acid (65%), are also able to convert native fibers to cellulose II.[43] Some atypical bacterial species are reported to biosynthesize cellulose II.[44]

Cellulose II exists in a monoclinic $P2_1$ phase (a = 8.10 Å, b = 9.03 Å, c = 10.31 Å, $\alpha = \beta = 90°$, and γ = 117.10°).[27,45,46] During conversion (I to II), the hydroxyl groups rotate from the *tg* to the *gt* conformation, which explicitly requires a change in the hydrogen-bond network.[47,48] In contrast to cellulose I, which has a parallel up arrangement, the chains in cellulose II are in an antiparallel arrangement yielding a more stable structure, which makes it preferable for various textiles and paper materials. The conversion of cellulose I to cellulose II has been widely considered irreversible, although (partial) regeneration of cellulose I from cellulose II has been reported.[49,50]

If cellulose I or II is exposed to ammonia (gas or liquefied) or various amines,[51] cellulose III is formed upon removal of the swelling agent. The resulting form of cellulose III depends on whether the starting form is I or II, giving rise to cellulose III_I or III_{II}. Their diffraction patterns are similar except for the meridional intensities. Cellulose III_I exists in a monoclinic $P2_1$ form (a = 4.450 Å, b = 7.850 Å, c = 10.31 Å, $\alpha = \beta = 90°$, and γ = 105.10°) with one chain in the unit cell, displaying parallel chains as observed in cellulose I.[52] However, the hydroxymethyl groups are in the *gt* conformation and the intersheet hydrogen bond network is similar to cellulose II. The exact structure of cellulose III_{II} is not clearly established yet, but the crystallographic and spectroscopic studies reported recently by Wada et al.[53] indicate that cellulose III_{II} is a disordered phase of cellulose. This disordered structure mainly contains a crystalline form having a unit cell (space group $P2_1$; a = 4.45 Å, b = 7.64 Å, c = 10.36 Å, $\alpha = \beta = 90°$, γ = 106.96°) occupied by one chain organized in antiparallel fashion, in addition to a second structure, as revealed by CP/MAS ^{13}C NMR (space group $P2_1$; a = 4.45 Å, b = 14.64 Å, c = 10.36 Å, $\alpha = \beta = 90°$, γ = 90.05°). Furthermore, either of these forms III_I or III_{II} reverts to its parent structure if placed in a high-temperature and humid environment.

Polymorphs IV_I and IV_{II} may be prepared by heating cellulose III_I or III_{II}, respectively, up to 260 °C in glycerol.[54,55] In a like manner to the case of cellulose III, these two forms can revert to the parent structures I or II. In addition to the native cellulose I, it has been shown that cellulose IV exists in several plant primary cell walls.[56,57]

3. Cellulose Nanocrystals

In the 1950s, Rånby reported for the first time that colloidal suspensions of cellulose can be obtained by controlled sulfuric acid-catalyzed degradation of cellulose fibers.[58−60] This work was inspired by the studies of Nickerson and Habrle[61] who observed that the degradation induced by boiling cellulose fibers in acidic solution reached a limit after a certain time of treatment. Transmission electron microscopy (TEM) images of dried suspensions revealed for the first time the presence of aggregates of needle-shaped particles, while further analyses of these rods with electron diffraction demonstrated that they had the same crystalline structure as the original fibers.[62,63] Simultaneously, the development by Battista[64,65] of the hydrochloric acid-assisted degradation of cellulose fibers derived from high-quality wood pulps, followed by sonification treatment, led to the commercialization of microcrystalline cellulose (MCC). Stable, chemically inactive, and physiologically inert with attractive binding properties, MCC offered a significant opportunity for multiple uses in pharmaceutical industry as a tablet binder, in food applications as a texturizing agent and fat replacer, and also, as an additive in paper and composites applications. After the acid hydrolysis conditions were optimized, Marchessault et al.[66] demonstrated that colloidal suspensions of cellulose nanocrystals exhibited nematic liquid crystalline alignment. Since the discovery of spectacular improvements in the mechanical properties of nanocomposites with cellulose nanocrystals,[67,68] substantial research has been directed to cellulose nanocrystal composites because of the growing interest in fabricating materials from renewable resources.

Cellulose nanocrystals are often referred to as microcrystals, whiskers, nanocrystals, nanoparticles, microcrystallites, or nanofibers. Hereafter, they are called "cellulose nanocrystals" (CNs). In the coming sections, methods for separation of CNs and their morphologies, characterization, modification, self-assembly, and applications will be reviewed.

3.1. Preparation of Cellulose Nanocrystals

The main process for the isolation of CNs from cellulose fibers is based on acid hydrolysis. Disordered or paracrystalline regions of cellulose are preferentially hydrolyzed, whereas crystalline regions that have a higher resistance to acid attack remain intact.[69,70] Thus, following an acid treatment that hydrolyzes the cellulose (leading to removal of the microfibrils at the defects), cellulose rod-like nanocrystals are produced. The obtained CNs have a morphology

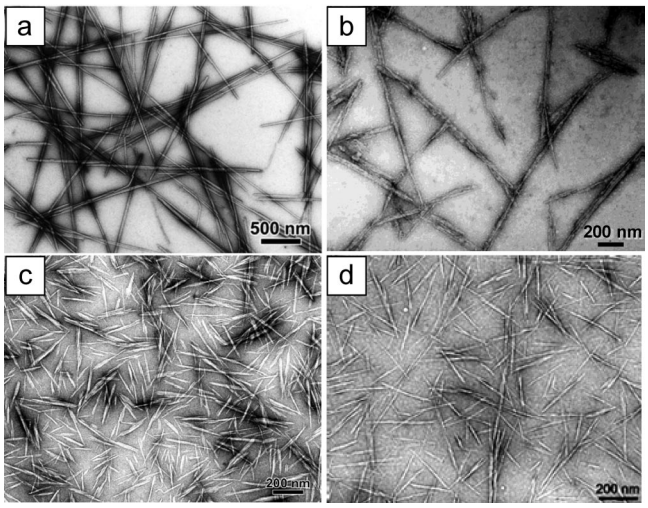

Figure 7. TEM images of dried dispersion of cellulose nanocrystals derived from (a) tunicate[79] (Reprinted with permission from ref 79. Copyright 2008 American Chemical Society), (b) bacterial[80] (Reprinted with permission from ref 80. Copyright 2004 American Chemical Society), (c) ramie[81] (From ref 81, Reproduced by permission of The Royal Society of Chemistry), and (d) sisal[82] (Reprinted with permission from ref 82. Copyright 2006 Springer).

and crystallinity similar to the original cellulose fibers; examples of such elements are given in Figure 7.

The actual occurrence of the acid cleavage event is attributed to differences in the kinetics of hydrolysis between amorphous and crystalline domains. In general, acid hydrolysis of native cellulose induces a rapid decrease in its degree of polymerization (DP), to the so-called level-off DP (LODP). The DP subsequently decreases much more slowly, even during prolonged hydrolysis times.[65,71−75] LODP has been thought to correlate with crystal sizes along the longitudinal direction of cellulose chains present in the original cellulose before the acid hydrolysis. This hypothesis was based on the reasonable assumption that disordered or para-crystalline domains are regularly distributed along the microfibers and therefore they are more susceptible to acid attack (in contrast to crystalline regions that are more impervious to attack). Also, homogeneous crystallites were supposed to be generated after acid hydrolysis. These assumptions were actually confirmed by X-ray crystal diffraction,[76] electron microscopy with iodine-staining,[76] small-angle X-ray diffraction,[72] and neutron diffraction analyses.[77] It was shown that the LODP values obtained by acid hydrolysis of cellulose correlated well with the periodic crystal sizes along cellulose chains. The value of LODP has been shown to depend on the cellulose origin, with typical values of 250 being recorded for hydrolyzed cotton,[64] 300 for ramie fibers,[77] 140−200 for bleached wood pulp,[65] and up to 6000 for the highly crystalline *Valonia* cellulose.[78] However, a wide distribution of DPs is typically observed for different cellulose sources, even at the LODP. Such a disparity in the quoted distributions stimulates vigorous discussion to the present day. In fact, the acid hydrolysis of bacterial, tunicate, *Valonia*, or cotton results in a higher polydispersity in the molecular weight, without any evidence of the LODP, probably because these cellulosic materials have no regular distribution of the less-organized domains.

Typical procedures currently employed for the production of CNs consist of subjecting pure cellulosic material to strong acid hydrolysis under strictly controlled conditions of temperature, agitation, and time. The nature of the acid and the acid-to-cellulosic fibers ratio are also important parameters that affect the preparation of CNs. A resulting suspension is subsequently diluted with water and washed with successive centrifugations. Dialysis against distilled water is then performed to remove any free acid molecules from the dispersion. Additional steps such as filtration,[79] differential centrifugation,[83] or ultracentrifugation (using a saccharose gradient)[84] have been also reported.

Specific hydrolysis and separation protocols have been developed that depend on the origin of the cellulosic fibers. Most common sources include among others, cellulose fibers from cotton,[85,86] ramie,[81,87,88] hemp,[89] flax,[90,91] sisal,[82,92] wheat straw,[93] palm,[94] bleached softwood[95] and hardwood[96] pulps, cotton linters pulp,[97,98] microcrystalline cellulose,[99−102] sugar beet pulp,[103] bacterial cellulose,[104−106] and Tunicates.[69,84,107]

Sulfuric and hydrochloric acids have been extensively used for CN preparation, but phosphoric[108−111] and hydrobromic[112] acids have also been reported for such purposes. If the CNs are prepared by hydrolysis in hydrochloric acid, their ability to disperse is limited and their aqueous suspensions tend to flocculate.[113] On the other hand, when sulfuric acid is used as a hydrolyzing agent, it reacts with the surface hydroxyl groups of cellulose to yield charged surface sulfate esters that promote dispersion of the CNs in water, resulting in important properties that will be discussed shortly.[114] However, the introduction of charged sulfate groups compromises the thermostability of the nanocrystals.[80] Also, differences in the rheological behavior have been shown between suspensions obtained from sulfuric acid hydrolysis and those obtained from hydrochloric acid. In fact, the sulfuric acid-treated suspension has shown no time-dependent viscosity, whereas the hydrochloric acid-treated suspension showed a thixotropic behavior at concentrations above 0.5% (w/v) and antithixotropic behavior at concentrations below 0.3%.[113] Post-treatment of CNs generated by hydrochloric acid hydrolysis with sulfuric acid has been studied to introduce, in a controlled fashion, sulfate moieties on their surfaces.[86,95] CNs generated from hydrochloric acid hydrolysis and then treated with sulfuric acid solution had the same particle size as those directly obtained from sulfuric acid hydrolysis; however, the surface charge density could be tuned to given values by sulfuric acid hydrolysis. With respect to the morphology of the particles, a combination of both sulfuric and hydrochloric acids during hydrolysis steps appears to generate spherical CNs instead of rod-like nanocrystals when carried out under ultrasonic treatment.[115,116] These spherical CNs demonstrated better thermal stability mainly because they possess fewer sulfate groups on their surfaces.[116]

The concentration of sulfuric acid in hydrolysis reactions to obtain CNs does not vary much from a typical value of ca. 65% (wt); however, the temperature can range from room temperature up to 70 °C and the corresponding hydrolysis time can be varied from 30 min to overnight depending on the temperature. In the case of hydrochloric acid-catalyzed hydrolysis, the reaction is usually carried out at reflux temperature and an acid concentration between 2.5 and 4 N with variable time of reaction depending on the source of the cellulosic material. Bondenson et al.[99,102] investigated optimizing the hydrolysis conditions by an experimental factorial design matrix (response surface methodology) using MCC that was derived from Norway spruce (*Picea abies*) as the cellulosic starting material. The factors that were varied during the process were the concentrations of MCC and

sulfuric acid, the hydrolysis time and temperature, and the ultrasonic treatment time. The responses that were measured were the median size of the cellulose particles and the yield of the reaction. The authors demonstrated that with a sulfuric acid concentration of 63.5% (w/w) over a time of approximately 2 h, it was possible to obtain CNs having a length between 200 and 400 nm and a width less than 10 nm with a yield of 30% (based on initial weight). Prolongation of the hydrolysis time induced a decrease in nanocrystal length and an increase in surface charge.[85] Reaction time and acid-to-pulp ratio on nanocrystals obtained by sulfuric acid hydrolysis of bleached softwood (black spruce, *Picea mariana*) sulfite pulp was investigated by Beck-Candanedo et al.[96] They reported that shorter nanoparticles with narrow size polydispersity were produced at longer hydrolysis times. Recently, Elazzouzi-Hafraoui et al.[79] studied the size distribution of CNs resulting from sulfuric acid hydrolysis of cotton treated with 65% sulfuric acid over 30 min at different temperatures, ranging from 45 to 72 °C. By increasing the temperature, they demonstrated that shorter crystals were obtained; however, no clear influence on the width of the crystal was revealed.

3.2. Morphology and Dimensions of Cellulose Nanocrystals

The geometrical dimensions (length, *L*, and width, *w*) of CNs are found to vary widely, depending on the source of the cellulosic material and the conditions under which the hydrolysis is performed. Such variations are due, in part, to the diffusion-controlled nature of the acid hydrolysis. The heterogeneity in size in CNs obtained from hydrolysis, for a given source type, can be reduced by incorporating filtration,[79] differential centrifugation,[83] or ultracentrifugation (using a saccharose gradient)[84] steps. The precise morphological characteristics are usually studied by microscopy (TEM, AFM, E-SEM,[117] etc.) or light scattering techniques, including small angle neutron scattering (SANS)[118] and polarized and depolarized dynamic light scattering (DLS, DDLS).[119] TEM images of CNs typically show aggregation of the particles, mainly due to the drying step for the preparation of the specimens after negative staining. Besides aggregation, additional instrumental artifacts usually lead to an overestimation of CN dimensions. To overcome these issues, Elazzouzi-Hafraoui et al.[79] recently reported the use of TEM in cryogenic mode (cryo-TEM) to prevent aggregation.

Atomic force microscopy (AFM) has been widely used to provide valuable and rapid indication of surface topography of CNs under ambient conditions at length scales down to the ångström level.[117,120−122] However, AFM topography may show rounded cross-sectional profiles in cases where other shapes are expected; for example, AFM imaging of *Valonia* gives shapes different than the square shape cross section observed under TEM. This is probably due to artifacts that result from substrate shape perturbations induced by AFM tip and tip-broadening effects. Finally, AFM was also reported to be a valuable technique to measure CNs mechanical properties and interactions, such as stiffness and adhesion or pull-off forces.[123]

Typical geometrical characteristics for CNs originating from different cellulose sources and obtained with a variety of techniques are summarized in Table 1. The reported width is generally approximately a few nanometers, but the length of CNs spans a larger window, from tens of nanometers to several micrometers. An arresting observation is that there is a direct correspondence between the length of the CNs and the LODP of the corresponding material because it is generally recognized that the rodlike CN consists of fully extended cellulose chain segments in a perfectly crystalline arrangement.

Table 1. Examples of the Length (*L*) and Width (*w*) of CNs from Various Sources Obtained by Different Techniques

source	*L* (nm)	*w* (nm)	technique	ref
bacterial	100−1000	10−50	TEM	105
	100−1000	5−10 × 30−50	TEM	80, 104
cotton	100−150	5−10	TEM	127
	70−170	∼7	TEM	128
	200−300	8	TEM	129
	255	15	DDL	119
	150−210	5−11	AFM	117
cotton linter	100−200	10−20	SEM-FEG	97
	25−320	6−70	TEM	79
	300−500	15−30	AFM	130
MCC	35−265	3−48	TEM	79
	250−270	23	TEM	101
	∼500	10	AFM	100
ramie	150−250	6−8	TEM	81
	50−150	5−10	TEM	131
sisal	100−500	3−5	TEM	82
	150−280	3.5−6.5	TEM	92
tunicate		8.8 × 18.2	SANS	118
	1160	16	DDL	119
	500−1000	10	TEM	107
	1000−3000	15−30	TEM	132
	100−1000	15	TEM	129
	1073	28	TEM	79
Valonia	>1000	10−20	TEM	125
soft wood	100−200	3−4	TEM	95, 113
	100−150	4−5	AFM	96
hard wood	140−150	4−5	AFM	96

CNs from wood are 3−5 nm in width and 100−200 nm in length, while those for *Valonia*, a sea plant, are reported to be 20 nm in width and 1000−2000 nm in length. Likewise, cotton gives CNs 5−10 nm in width and 100−300 nm long, and tunicate, a sea animal, gives ca. 10−20 nm in width and 500−2000 nm long.[69] The aspect ratio, defined as the length-to-width (*L*/*w*) spans a broad range and can vary between 10 and 30 for cotton and ca. 70 for tunicate.

The morphology of the cross section of CNs also depends on the origin of the cellulose fibers. The basis of the morphological shape in the cross section may be attributed to the action of the terminal complexes during cellulose biosynthesis. In fact, depending on the biological origin of the cell wall, different arrangements of TCs have been observed, which generate cellulose crystals with different geometries.[14] Despite the fact that acid hydrolysis appears to erode the crystal by preferentially peeling off angular cellulose sheets, as has been reported by Helbert et al.,[124] a number of analyses of cross sections of CNs have nevertheless attempted to characterize the inherent CN geometry. Based on TEM observations, Revol[125] reported that the cross section of cellulose crystallites in *Valonia ventricosa* was almost square, with an average lateral element length of 18 nm. In contrast, CNs from tunicate that were analyzed by TEM[126] and SANS were found to have a rectangular 8.8 nm × 18.2 nm cross-sectional shape.[118]

The morphology of CNs along the axis of the crystal seems to also present different features, depending on the source of the nanocrystal. CNs from bacterial cellulose[121] and tunicate[79] have been reported to have ribbon-like shapes with twists having half-helical pitches of 600−800 nm (*Micrasterias denticulata*) and 1.2−1.6 μm, respectively. However,

these twisted features have not been clearly evidenced in CNs extracted from higher plants, which are believed to be flat with uniplanar-axial orientation.

4. Chemical Modifications of Cellulose Nanocrystals

Because of a natural advantage of an abundance of hydroxyl groups at the surface of CNs, different chemical modifications have been attempted, including esterification, etherification, oxidation, silylation, polymer grafting, etc. Noncovalent surface modification, including the use of adsorbing surfactants and polymer coating, has been also studied. All chemical functionalizations have been mainly conducted to (1) introduce stable negative or positive electrostatic charges on the surface of CNs to obtain better dispersion (CNs obtained after sulfuric acid hydrolysis introduce labile sulfate moieties that are readily removed under mild alkaline conditions) and (2) tune the surface energy characteristics of CNs to improve compatibility, especially when used in conjunction with nonpolar or hydrophobic matrices in nanocomposites. The main challenge for the chemical functionalization of CNs is to conduct the process in such a way that it only changes the surface of CNs, while preserving the original morphology to avoid any polymorphic conversion and to maintain the integrity of the crystal.

4.1. Noncovalent Surface Chemical Modifications

Noncovalent surface modifications of CNs are typically made via adsorption of surfactants. This approach has been introduced by Heux et al.,[129,133] who used surfactants consisting of the mono- and di-esters of phosphoric acid bearing alkylphenol tails. The obtained surfactant-coated CNs dispersed very well in nonpolar solvents.[129] Detailed analyses

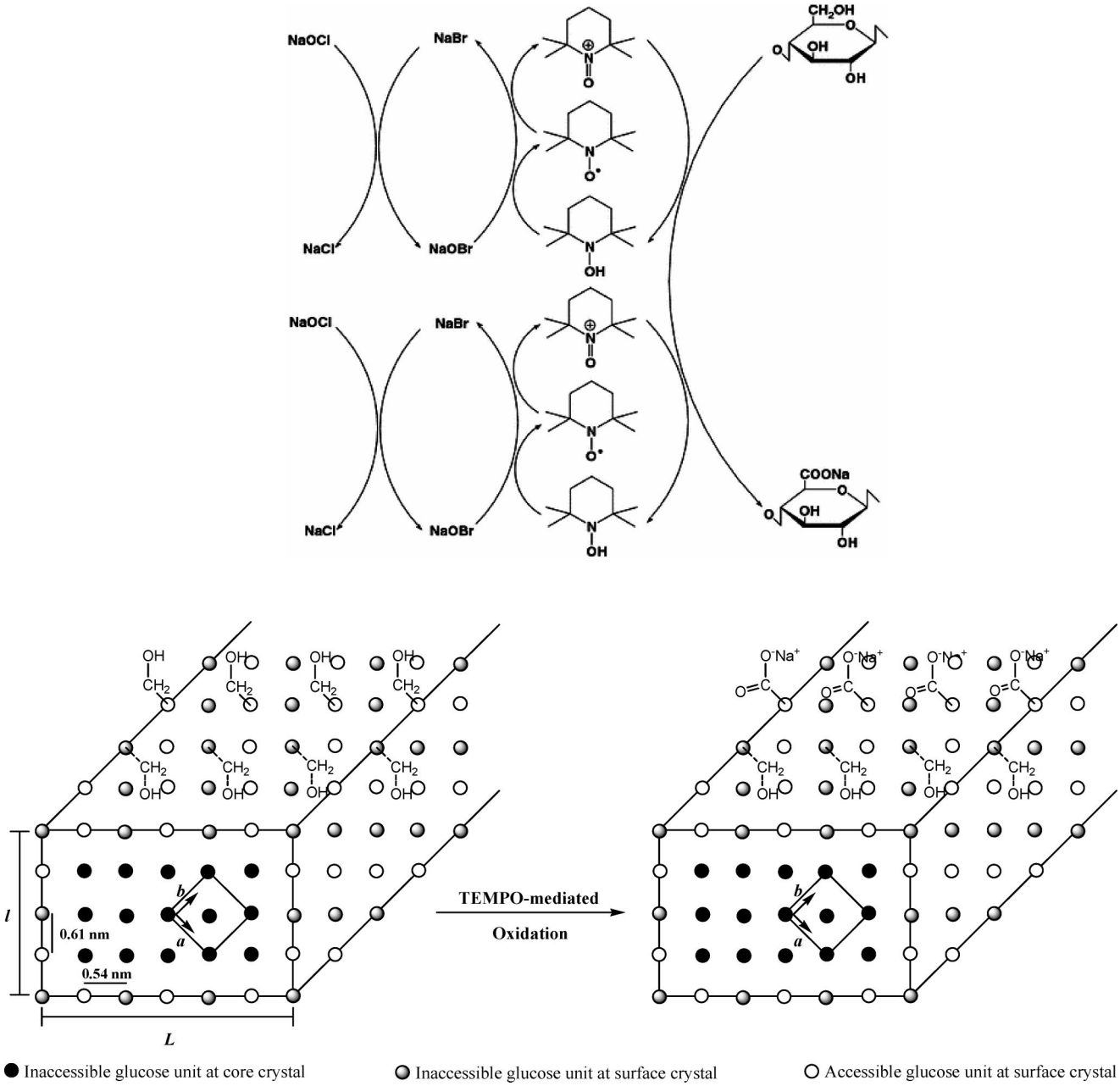

Figure 8. Scheme of TEMPO-mediated oxidation mechanism of the hydroxymethyl groups of cellulose (top, reaction scheme) and cross-sectional representation of cellulose nanocrystal indicating the occurrence of the surface TEMPO-mediated oxidation of available hydroxyl groups (bottom, surface crystal representations).

of the data provided by SANS revealed that the surfactant molecules formed a thin layer of about 15 Å at the surface of the CNs.[134] When the surface-modified CNs were incorporated into isotactic polypropylene, they showed very good compatibility and they acted as remarkable nucleating agents to induce the formation of the rare β crystalline form in addition to the regular crystalline form of isotactic polypropylene α.[135,136] An anionic surfactant was also used by Bondeson et al.[137] to enhance the dispersion of CNs in poly(lactic acid) (PLA). Kim et al.[138] and Rojas et al.[139] used nonionic surfactants to disperse CNs in polystyrene-based composite fibers. Zhou et al.[140] recently reported a new and elegant way of CN surface modification based on the adsorption of saccharide-based amphiphilic block copolymers. By mimicking lignin−carbohydrate copolymers, they adsorbed xyloglucan oligosaccharide−poly(ethylene glycol)−polystyrene triblock copolymer onto the surface of CNs. The resulting CNs showed excellent dispersion abilities in nonpolar solvents.

4.2. TEMPO-Mediated Oxidation

(2,2,6,6-Tetramethylpiperidine-1-oxyl)-mediated (or TEMPO-mediated) oxidation of CNs has been used to convert the hydroxylmethyl groups present on their surface to their carboxylic form. This oxidation reaction, which is highly discriminative of primary hydroxyl groups, is also "green" and simple to implement. It involves the application of a stable nitroxyl radical, the 2,2,6,6-tetramethylpiperidine-1-oxyl (TEMPO), in the presence of NaBr and NaOCl (see Figure 8, top). The use of this technique has been the subject of a number of reports since it was first introduced by De Nooy et al.,[141] who showed that only the hydroxymethyl groups of polysaccharides were oxidized, while the secondary hydroxyls remained unaffected. In fact, TEMPO-mediated oxidation of CNs involves a topologically confined reaction sequence, and as a consequence of the 2-fold screw axis of the cellulose chain, only half of the accessible hydroxymethyl groups are available to react, whereas the other half are buried within the crystalline particle (Figure 8, bottom).

TEMPO-mediated oxidation of CNs, obtained from HCl hydrolysis of cellulose fibers, was first reported by Araki et al.[127] as an intermediate step to promote grafting of polymeric chains. These authors demonstrated that after TEMPO-mediated oxidation, the CNs maintained their initial morphological integrity and formed a homogeneous suspension when dispersed in water. The basis for these latter observations was the presence of the newly installed carboxyl groups that imparted negative charges at the CN surface and thus induced electrostatic stabilization. Similar observations were reported by Montanari et al.[142] who also showed that during excessive TEMPO-mediated oxidation, a decrease of the crystal size occurred resulting from the partial delamination of cellulose chains that are extant on the surface.

Habibi et al.[143] performed TEMPO-mediated oxidation of CNs obtained from HCl hydrolysis of cellulose fibers from tunicate and showed that it did not compromise the morphological integrity of CNs or their native crystallinity. On the basis of the supramolecular structure, morphology, and crystallographic parameters of the CNs, these authors demonstrated that various degrees of oxidation can be predicted and achieved by using specific amounts of the primary oxidizing agent, that is, NaOCl (see Figure 8, bottom). When dispersed in water, TEMPO-oxidized or carboxylated CN suspensions display birefringence patterns and do not flocculate or sediment owing to the polyanionic character imparted by the negative charges on the CNs surfaces (see Figure 9).

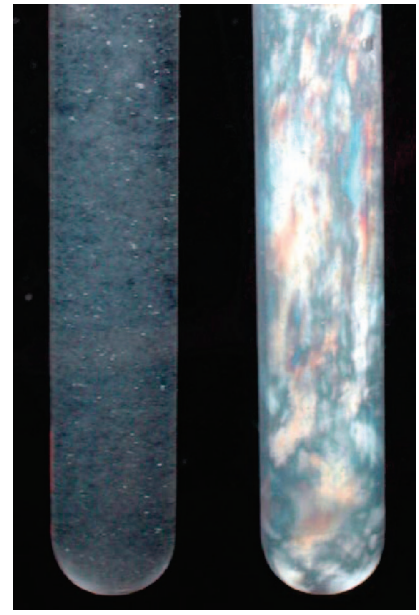

Figure 9. Aqueous 0.53% (w/v) suspensions of cellulose nanocrystals observed between crossed polarizers (1) after production by HCl-catalyzed hydrolysis (left) and (2) after their oxidation via TEMPO-mediated reactions (right). Reprinted with permission from ref 143. Copyright 2006 Springer.

4.3. Cationization

Positive charges can also be easily introduced on the surface of CNs; for example, weak or strong ammonium-containing groups, such as epoxypropyltrimethylammonium chloride (EPTMAC), can be grafted onto the CN surfaces.[144] Such surface cationization proceeds via a nucleophilic addition of the alkali-activated cellulose hydroxyl groups to the epoxy moiety of EPTMAC and leads to stable aqueous suspensions of CNs with unexpected thixotropic gelling properties. Shear birefringence was observed, but no liquid crystalline chiral nematic phase separation was detected for these cationic CNs, most likely owing to the high viscosity of the suspension.

4.4. Esterification, Silylation and Other Surface Chemical Modifications

Homogeneous and heterogeneous acetylation of model CNs extracted from *Valonia* and tunicate has been studied by Sassi and Chanzy by using acetic anhydride in acetic acid.[126] Their ultrastructural study, carried out by TEM imaging and X-ray diffraction, showed that the reaction proceeded by a reduction of the diameters of the crystals, while only a limited reduction in CN length was observed. It has been suggested that the reaction involved a nonswelling mechanism that affected only the cellulose chains localized at the crystal surface. In the case of homogeneous acetylation, the partially acetylated molecules immediately partitioned into the acetylating medium as soon as they were sufficiently soluble, while in heterogeneous conditions, the cellulose acetate remained insoluble and surrounded the crystalline core of unreacted cellulose chains. The simultaneous occurrence of cellulose hydrolysis and acetylation of hydroxyl

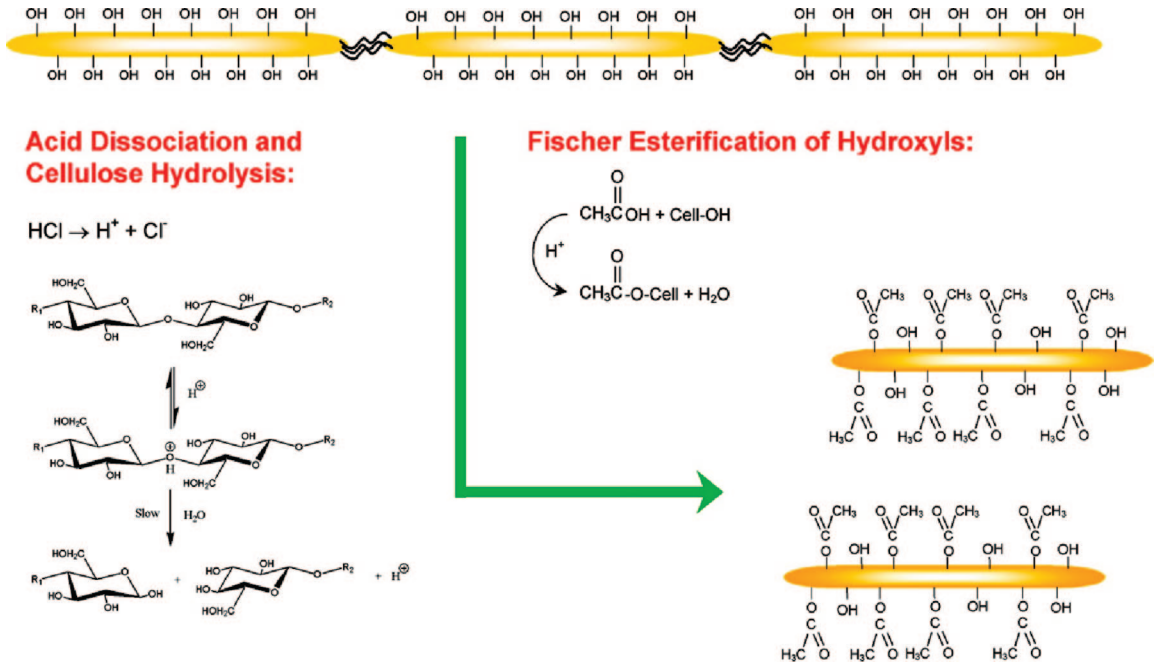

Figure 10. Reaction scheme illustrating the one-pot (tandem) cellulose hydrolysis and esterification reactivity of hydroxyl groups. Reprinted with permission from ref 145. Copyright 2009 American Chemical Society.

groups has been also reported. Fischer esterification of hydroxyl groups simultaneously with the hydrolysis of amorphous cellulose chains has been introduced as a viable one-pot reaction methodology that allows isolation of acetylated CNs in a single-step process (Figure 10).[145,146]

An environmentally friendly CN surface acetylation route was recently developed by Yuan et al.[147] involving a low reagent consumption and simple-to-apply procedure. The method used alkyenyl succinic anhydride (ASA) aqueous emulsions as a template. The emulsions were simply mixed with CN suspensions and freeze-dried, and the resulting solid was heated to 105 °C. The obtained derivative conferred to the acylated CNs a highly hydrophobic character that was evident because they were easily dispersible in solvents with widely different polarities as measured by the respective dielectric constant, ε; for example, they were dispersible not only in DMSO having a very high ε of 46.45 but also in 1,4-dioxane that has a quite low ε of 2.21. Berlioz et al.[148] have reported recently a new and highly efficient synthetic method for an almost complete surface esterification of CNs, leading to highly substituted CN esters. The reaction of fatty acid chains was carried out on dried CNs via a gas-phase process. It has been shown by SEM and X-ray diffraction analyses that the esterification proceeded from the surface of the substrate to the crystal core. Under moderate conditions, the surface was fully reacted, whereas the original morphology was maintained and the core of the crystal remained unmodified. Esterification of CNs by reacting organic fatty acid chlorides, having different lengths of the aliphatic chain (C_{12} to C_{18}), has also been reported with a grafting density high enough that the fatty acids with backbones of 18 carbons were able to crystallize on the surface of the CNs.[131]

Cellulose whiskers resulting from the acid hydrolysis of tunicate have been partially silylated by a series of alkyldimethylchlorosilanes, with the carbon backbone of the alkyl moieties ranging from a short carbon length of isopropyl to longer lengths represented by *n*-butyl, *n*-octyl, and *n*-dodecyl.[149] It has been demonstrated that with a degree of substitution (DS) between 0.6 and 1, the whiskers became readily dispersible in solvents of low polarity (such as THF) leading to stable suspensions with birefringent behavior, while their morphological integrity was preserved. However, at high silylation (DS greater than 1), the chains in the core of the crystals became silylated, resulting in the disintegration of the crystals and consequently the loss of original morphology. Surface trimethyl silylation of CNs from bacterial cellulose and their resulting cellulose acetate butyrate[104,150] or polysiloxane[151] based nanocomposites was also investigated by Roman and Winter. Finally, coupling CNs with *N*-octadecyl isocyanate, via a bulk reaction in toluene, has also been reported to enhance their dispersion in organic medium and compatibility with polycaprolactone, which significantly improved the stiffness and ductility of the resultant nanocomposites.[92]

4.5. Polymer Grafting

Polymer grafting on the surface of CNs has been carried out using two main strategies, namely, the "grafting-onto" and "grafting-from".[152] The grafting onto approach involves attachment onto hydroxyl groups at the cellulose surface of presynthesized polymer chains by using a coupling agent. In the "grafting from" approach, the polymer chains are formed by *in situ* surface-initiated polymerization from immobilized initiators on the substrate.

The "grafting onto" approach was used by Ljungberg et al.[153] to graft maleated polypropylene (PPgMA) onto the surface of tunicate-extracted CNs. The resulting grafted nanocrystals showed very good compatibility and high adhesion when dispersed in atactic polypropylene. Araki et al.[127] and Vignon et al.[154] studied the grafting of amine-terminated polymers on the surface of TEMPO-mediated oxidized CNs by using a peptide coupling process catalyzed by carbodiimide derivatives in water. The same approach has been implemented by Mangalam et al.[155] who grafted DNA oligomers on the surface of CNs. The grafting of polycaprolactone having different molecular weights on the

surface of CNs has been achieved by using isocyanate-mediated coupling.[87] These authors reported reaching a grafting density that was high enough that the grafted PCL chains were able to crystallize at the surface of CNs. Similar efforts were made by Cao et al.[98] who reported the isocyanate-catalyzed grafting of presynthesized water-borne polyurethane polymers via a one-pot process. Such crystallization provoked cocrystallizations of the free chains of the respective polymer matrices during CN-based nanocomposite processing. Furthermore, this cocrystallization phenomenon induced the formation of a co-continuous phase between the matrix and filler, which significantly enhanced the interfacial adhesion and consequently contributed to a highly improved mechanical strength of the resulting nanocomposites.

The "grafting from" approach applied to CNs was first reported by Habibi et al.,[81] who grafted polycaprolactone onto the surface of CNs via ring-opening polymerization (ROP) using stannous octoate ($Sn(Oct)_2$) as a grafting and polymerization agent. Likewise, Chen et al.[156] and Lin et al.[157] conducted similar grafting reactions under microwave irradiation to enhance the grafting efficiency. *In situ* polymerization of furfuryl alcohol from the surface of cellulose whiskers was studied by Pranger et al.[100] In this case, the polymerization was catalyzed by sulfonic acid residues from the CN surface. At elevated temperatures, the sulfonic acid groups were de-esterified and consequently released into the medium to catalyze *in situ* the polymerization. Yi et al.[158] and Morandi et al.[159] propagated polystyrene brushes via atom transfer radical polymerization (ATRP) on the surface of CNs with ethyl 2-bromoisobutyrate as the initiator agent. Similarly, other vinyl monomers, mainly acrylic monomers such as *N*-isopropylacrylamide, were also polymerized from the surface of CNs to produce thermoresponsive substrates.[160,161] Grafting of polyaniline from CNs was achieved by *in situ* polymerization of aniline onto CNs in hydrochloric acid aqueous solution, via an oxidative polymerization using ammonium peroxydisulfate as the initiator.[162]

5. Self-Assembly and -Organization of Cellulose Nanocrystals

When sulfuric acid is used as the hydrolyzing agent, it also chemically reacts with the surface hydroxyl groups of CNs to yield negatively charged (surface) sulfate groups that promote a perfectly uniform dispersion of the whiskers in water via electrostatic repulsions.[114] By inference, continuous removal of the water phase should therefore tend to cause the nanocrystals to adopt configurations that minimize the existing electrostatic interactions. Indeed, (homogeneous) concentrated suspensions self-organize into spectacular liquid crystalline arrangements, a phenomenon similar to what occurs in nonflocculating suspensions of other rod-like particles, such as poly(tetrafluoroethylene) whiskers,[163] tobacco mosaic viruses (TMV),[164] DNA fragments,[165] or crystallites extracted from other polysaccharides such as chitin.[166]

This self-organization phenomenon was revealed by the appearance of "fingerprint" patterns obtained from suspensions observed by polarized optical microscopy, indicative of a chiral-nematic ordering.[114] An even more striking finding is that this chiral nematic structure can be preserved after complete water evaporation to provide iridescent films of CNs. These solid films, in addition to allowing fundamental studies of their striking behavior, have numerous potential applications such as coating materials for decorative materials and security papers (because the optical properties cannot be reproduced by printing or photocopying).[167]

An investigation into these systems reveals that CNs are randomly oriented in the dilute regime (isotropic phase). Indeed, polarized optical microscopy demonstrates that at dilute concentrations, CNs appear as spheroids or ovaloids and the initial ordered domains are similar to tactoids. A nematic liquid crystalline alignment is adopted when the CN concentration increases because these tactoids coalesce to form an anisotropic phase, which is characterized by a unidirectional self-orientation of the CN rods. When the suspension reaches a critical concentration of CNs, it forms a chiral nematic ordered phase displaying lines that are the signature of cholesteric liquid crystals (see Figure 14). Above the critical concentration of chiral nematic phase formation, aqueous CN suspensions produce shear birefringence, and on standing, they can spontaneously separate into an upper isotropic and a lower anisotropic phase (Figure 11).

These chiral nematic or cholesteric structures in the anisotropic phase consist of stacked planes of CN rods aligned along a vector (director), with the orientation of each director rotated about the perpendicular axis from one plane to the next as shown in Figure 11. The self-induced parallel alignment phenomenon of the CNs that occurs above a critical concentration is attributed to the well-known entropically driven self-orientation phenomenon of rod-like

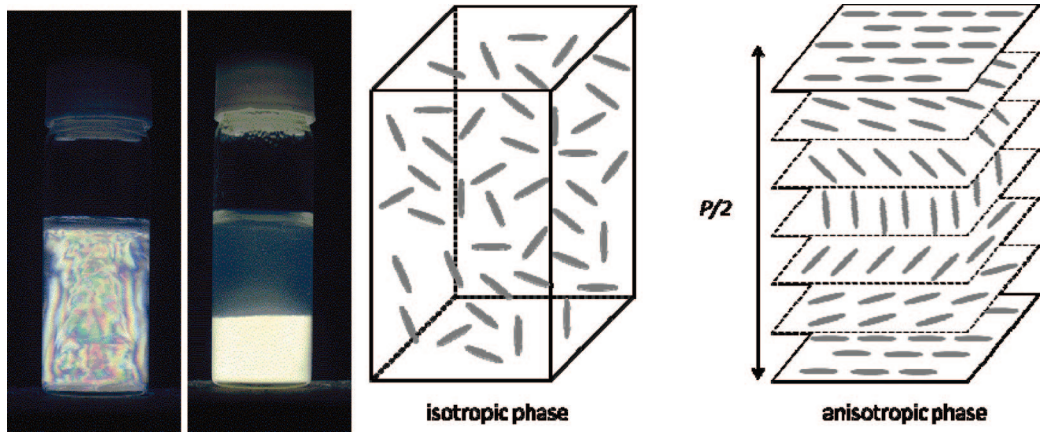

Figure 11. (left) Aqueous 0.63% (w/w) CN suspension observed between crossed polarizers. Immediately after shearing the suspension shows many iridescent birefringence patterns; after 1 week, the suspension separates into the upper isotropic and the lower anisotropic phases (Reprinted with permission from ref 105. Copyright 2001 American Chemical Society). (right) Schematic representation of CN orientation in both the isotropic and anisotropic (chiral nematic) phases.

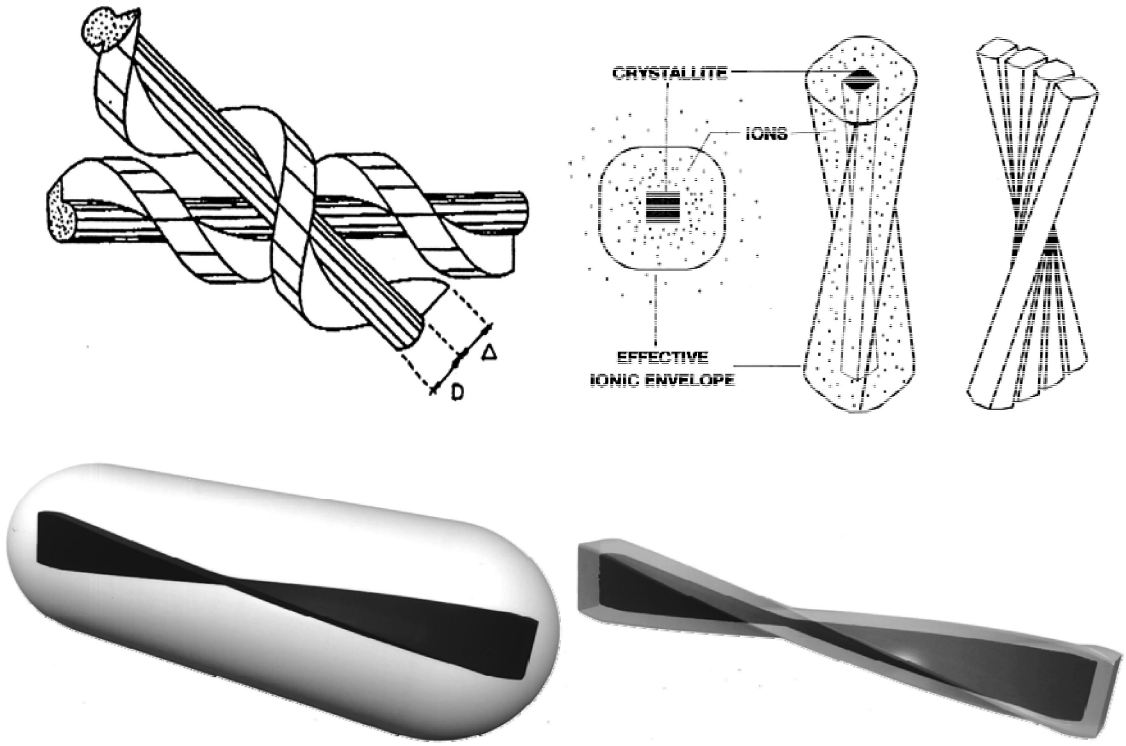

Figure 12. (top) Representations suggested by Orts et al. for the tighter packing achievable by the chiral interaction of twisted rods: left, the distance between rods is reduced to *D* if instead of rods packing with axes parallel they pack with the "thread" of one rod fitting into the "groove" of its neighbor; (right) for nanocrystals with an electrostatic double layer, a threaded rod would alter the surrounding electric double layer and affect packing over relatively large distances (Reprinted with permission from ref 170. Copyright 1998 American Chemical Society). (bottom) Schematic illustration of bacterial cellulose nanocrocrystals with surface charge, showing the change in effective particle shape: (left) in water, repulsion by surface charge extends to long-range, resulting in an apparently nonchiral rod; (right) addition of NaCl decreases repulsion range and the effective particle becomes a twisted rod (Reprinted with permission from ref 105. Copyright 2001 American Chemical Society).

species to give nematic order. Its origin can be attributed to favorably excluded volume interactions leading to higher packing entropy compared with the disordered phase.

The origin of this spontaneous self-assembly phenomenon was proposed to be akin to the helicoidal structures often observed in naturally occurring materials containing cellulose.[114,168,169] Because of the absence of any structural chirality in the molecules in these suspensions, this helicoidal arrangement was assumed to be due to an asymmetry that induces chiral nematic packing. Revol and Marchessault hypothesized that there must be a twist in the CNs themselves that accounts for their chiral interaction.[166] Thus, because suspensions of uncharged CNs, generated from HCl, do not give rise to such chiral nematic order, negative charges from ionized sulfate groups on the surface of CNs were thought to be imperative for phase stability, and their helical distribution has also been suggested to be the "twisting agent".[114] However, recent studies carried out on suspensions in which CNs were sterically stabilized by surfactant coating[129] or polymer grafting[127] provided more evidence of twists in the CN nanostructure. In fact, it has been found that even if electrostatic repulsions are screened after rudimentary adsorption or grafting modifications to the CNs, the suspensions conserve their chiral nematic order.[127,129] Orts et al.[170] have confirmed, based on *in situ* small angle neutron scattering (SANS) measurements of CNs in aqueous suspension (under magnetic field and shear alignment), the hypothesis that CNs are screw-like rods (Figure 12, top). More supporting evidence was reported by Araki and Kuga[105] who showed that surprisingly, CNs from bacterial cellulose form a nonchiral nematic phase in an electrolyte-free suspension, whereas in the presence of an electrolyte, the suspension assumes chiral nematic order. This phenomenon was explained by nontrivial morphological changes in the CN, that is, from a plain cylindrical configuration to a twisted rod, as a result of the screening of surface charge (Figure 12, bottom). In fact, the dilatation of CNs resulting from the repulsive force by surface charges would obscure the chiral morphology, making the effective rods straight and smooth; permitting this configuration to lead to the formation of a nematic phase by parallel packing of these rods. Addition of an electrolyte would induce shrinkage of the effective particle size; in this scenario, the twisted morphology manifests itself in mutual alignment of the rods and results in the formation of chiral nematic order (Figure 12 bottom).

The concept of ordered chiral nematic phases and their properties such as those observed in CN suspensions has been shown to be dictated by classical phase equilibrium theories related to colloidal liquid crystals such as the Onsager theory[171] or its extended version such as the Stroobants, Lekkerkerker, and Odijk (SLO) theory.[172] The phase-forming ability depends on several parameters such as the aspect ratio of the particles, the charge density, and the osmotic pressure.

5.1. Self-Assembly and -Organization of CNs in Aqueous Medium

The critical concentration of sulfated CNs necessary for the formation of ordered nematic phases in electrolyte-free aqueous suspensions depends to a large degree on the charge density and typically ranges between 1% and 10% (w/w). The resultant chiral nematic anisotropic phases typically

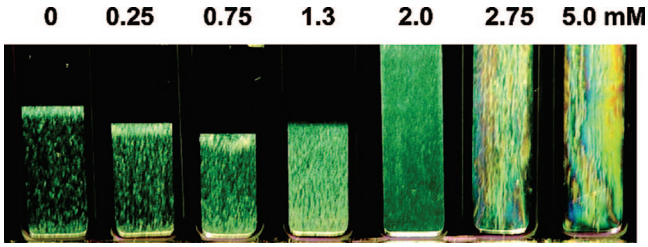

Figure 13. Effect of added NaCl on the phase behavior of suspensions of CNs from bacterial cellulose for a fixed total cellulose concentration of 3 wt % after 25 days of standing. Reprinted with permission from Ref 106. Copyright 2009 American Chemical Society.

display a pitch that decreases with increasing CN concentration and can vary from 20 to 80 μm.

The isotropic-to-anisotropic (chiral nematic phase) equilibrium is sensitive to the presence of electrolytes and the specific nature of the electrolyte counterions. Quantitative studies of the changes in composition of the isotropic and anisotropic phases as a function of electrolyte concentration where both phases coexist,[128] as well as the effect of the type of counterion,[173] have been conducted. It has been found from the latter study that increasing the amount of added electrolyte decreases anisotropic phase formation. Interestingly, the chiral nematic pitch was found to decrease, that is, the phase became more highly twisted, as the electrolyte concentration increased. Apparently, the decrease in pitch occurred because the decrease in the electrical double layer thickness increased the chiral interactions between the crystallites.[128] As already indicated, the phase separation of sulfated CN suspensions also depends strongly on the nature of their counterions.[173] For inorganic counterions, the critical concentration for ordered phase formation increases in general as a function of increasing van der Waals' radii, in the order $H^+ < Na^+ < K^+ < Cs^+$. For organic counterions such as NH_4^+, $(CH_3)_4N^+$, $(CH_3CH_2)_4N^+$, $(CH_3CH_2CH_2)_4N^+$, $(CH_3CH_2CH_2CH_2)_4N^+$, $(CH_3)_3HN^+$, and $(CH_3CH_2)_3HN^+$, the critical concentration depends on the relative contributions of hydrophobic attraction and steric repulsion. In general, most of the work in this area has demonstrated that the critical concentration increases with increasing counterion size. It was also found that the chemical nature of the counterions also influences the stability, the temperature dependence of the phase separation, the chiral nematic pitch, and the redispersibility of dried samples made from the suspensions.

Sulfuric acid-hydrolyzed CNs obtained from bacterial cellulose have been reported to spontaneously separate in a nematic phase.[105] This phase separation event is preceded by a birefringent glass-like state that can persist for up to 7 days. However, adding a trace electrolyte (<1 mM NaCl) caused separation in 2 days and permitted the anisotropic phase to become chiral nematic.[105] The presence of an electrolyte also significantly decreased the volume of the lower anisotropic phase.[105] A detailed examination of this unexpected phase separation and the effect of NaCl (at high salt concentrations, up to 5 mM) was recently conducted by Hirai et al.[106] They reported that the volume fraction of the chiral nematic phase displayed a minimum at a NaCl concentration of ca. 1.0 mM. If the NaCl concentrations were varied over the range of 2.0−5.0 mM, no phase separation occurred, but the suspensions became completely liquid crystalline (Figure 13). The size of the ordered domains in the anisotropic phase decreased with NaCl concentration in the range from 0 to 2.75 mM. At 2.75 mM, only tactoids were observed, whereas at 5.0 mM, chiral nematic domains were no longer observed. In addition, the chiral nematic pitch decreased with increasing NaCl concentration from ~16.5 μm for electrolyte-free suspension to a minimum value of 12 μm at approximately 0.75 mM and finally increased sharply to greater than 19 μm at concentrations up to 2.0 mM.

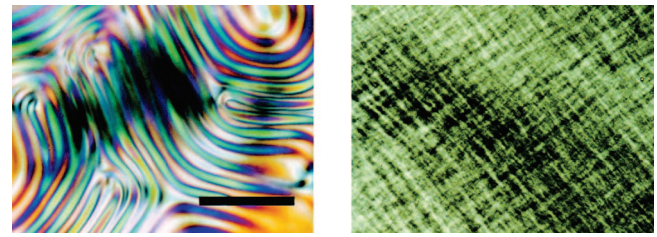

Figure 14. Polarized-light micrographs of CN suspensions: (left) fingerprint pattern in the chiral nematic phase of the directly H_2SO_4-hydrolyzed suspension (initial solid content, 5.4%); (right) crosshatch pattern of postsulfated suspension (solid content, 7.1%). Reprinted with permission from ref 86. Copyright 2000 American Chemical Society.

Similarly to electrolytes, the effect of (nonadsorbing) macromolecules, such as blue dextran or ionic dyes, was reported by Beck-Candanedo et al.[174−176] to induce an entropic phase separation of aqueous suspensions of anisotropic sulfuric-acid-hydrolyzed CNs to an isotropic phase. Anionic dyes induced phase separation at much lower ionic strengths than simple 1:1 electrolytes (e.g., NaCl), likely because of their polyvalent character and larger hydration radius. However, it has been shown that the electrostatic attraction and chemical binding of cationic and anionic dyes appear to inhibit phase separation in the CN suspensions.[174] It has also been demonstrated that when anionic dyes are attached to nonadsorbing macromolecules such as dextran, a triphase isotropic−isotropic−nematic equilibrium is obtained. This peculiar behavior was observed also with neutral blue dextran; the concentration of dextran needed to produce the triphase equilibrium appeared to be strongly influenced by its molecular weight or charge density.[176] The mechanism of the phase behavior of these suspensions seemed to be governed by both repulsive electrostatics and attractive entropic forces: the presence of anionic dyes raised the ionic strength of the system, and at low ionic strength, a larger amount of CNs was needed to reach the critical cellulose concentration required for phase separation, shifting the phase equilibrium into the region of isotropic−chiral nematic phase coexistence. At higher ionic strengths, the electrostatic repulsions between the rods were sufficiently screened to allow depletion attractions from the dextran macromolecules and produce phase separation.[175]

The nature and density of the charges on the surface of CNs have also been reported to affect the formation of the chiral nematic phase. By using post-sulfated HCl-hydrolyzed CNs, which have a sulfur content approximately one-third less than directly H_2SO_4-hydrolyzed CNs, Araki et al.[86] reported distinctly different behaviors. Indeed, post-sulfonated suspensions formed a birefringent glassy phase having a crosshatch pattern (Figure 14) rather than a fingerprint pattern indicative of chiral nematic phases typical of directly sulfated CNs (Figure 14). Interestingly, a high viscosity suspension of postsulfated CNs does not yield a chiral nematic phase most likely due to its low charge content.

Carboxylated CNs, prepared by TEMPO-mediated oxidation, have been shown to form homogeneous dispersions in water that are strongly birefringent. This shear birefringence was not uniformly distributed throughout the system, but consisted instead of domains of various sizes and colors indicative of local domain orientation within the CNs that never reached the chiral nematic order in the form of either tactoids or fingerprints. The lack of further organization was ascribed to the high polydispersity among the length of the CNs (that were obtained from tunicate by HCl acid prehydrolysis) and to the high viscosity of the suspensions.[143] However, when carboxylated CNs were prepared from cotton fibers, a reduced CNs' length polydispersity was observed, and thus, these suspensions reached a chiral nematic order with a pitch of 7 μm at a concentration of 5% or more (w/w). Furthermore, when PEG was grafted on the surface of the CNs, the resulting PEG-grafted CNs gave rise to a chiral nematic mesophase through a phase separation similar to that of the unmodified CNs, but with a reduced spacing of the fingerprint pattern (around 4.0 μm).[127] Moreover, unlike what has been previously found, PEG-grafted CNs showed drastically enhanced dispersion stability even at high solid content and the ability to redisperse into either water or chloroform from a freeze-dried state. They also demonstrated strong stability at high ionic strength because of a reduced electroviscous effect, and no aggregations were observed upon addition of electrolyte up to 2 M NaCl.

Shear birefringence was also observed for suspensions of cationic epoxypropyltrimethylammonium chloride-grafted CNs, but no liquid crystalline chiral nematic phase separation was detected, most likely because the phase was inhibited as a result of the high viscosity of the suspension.[144]

5.2. Self-Assembly and -Organization of CNs in Organic Medium

Heux et al.[129] provided the first description of a self-ordering phenomenon for CNs in apolar solvents. In their preliminary study, surfactant coating was used to disperse CNs and thereby obtain a chiral-nematic structure. However, the pitch of the chiral nematic structure was found to be approximately 4 μm, a value that is too small compared with the case of aqueous suspensions (pitch between 20 and 80 μm). In addition, higher CN concentrations, up to 36%, could be achieved. These results were attributed to the steric stabilization exerted by the surfactant coating. In fact, this stabilization screened out the electrostatic repulsion and consequently induced stronger chiral interactions between rods that ultimately allowed for higher packing. Detailed examination of the structure of this chiral nematic phase has been reported recently by the same group.[177,178] They studied the correlation of the aspect ratio of CNs extracted from cotton fibers and their dispersion in an apolar solvent such as cyclohexane. The critical concentration in which spontaneous phase separation into a chiral nematic mesophase was observed was higher than that in water. Correlation with Onsager's theory for these organophilic suspensions was not possible because the experimental critical concentrations were much lower than the predicted ones, probably due to an attractive interaction between the rods in the apolar medium. These strong interactions also induced a decrease in the chiral nematic pitches that were of the order of 2 μm or less. In addition, suspensions prepared with CNs having high aspect ratios did not show any phase separation but instead produced an anisotropic gel phase at a high concentration.[177] Conversely, the chiral nematic pitch was much larger ($\sim$17 μm) for suspensions of CNs in toluene that were stabilized by xyloglucan oligosaccharide−poly(ethylene glycol)−polystyrene triblock copolymer.[140]

5.3. Self-Assembly and -Organization of CNs under External Fields

Nonflocculated CNs in an aqueous suspension under an external field, whether magnetic or electric, can be oriented. They can orient when they are subjected to a magnetic field due to the negative diamagnetic anisotropy of cellulose. Although the diamagnetic anisotropy of cellulose is relatively weak per molecular repeat unit, the cellulose rod-like nanocrystals are long and heavy, so their total diamagnetic anisotropy is rather larger compared with other particles such DNA or TMV.[179,180] Sugiyama et al.[180] first demonstrated that dilute aqueous suspensions of crystalline cellulose extracted from tunicate were able to orient when subjected to a magnetic field of 7 T. Films were obtained in which the crystals were oriented with their long axes perpendicular to the magnetic field. An overall gross CN orientation could be achieved where the cholesteric axis became parallel to the magnetic field rather than unwinding the chiral nematic structure. Fleming et al. demonstrated that the orientation of a liquid crystalline CN suspension in the magnetic field of a NMR spectrometer can assist in interpretation of the NMR spectra of proteins added to the suspension.[181] Recently, Kimura et al.[132] showed that the chiral nematic behavior of CN suspensions could be unwound by applying a slowly rotating strong magnetic field. Kvien and Oksman attempted to align CNs in a polymer matrix (e.g., polyvinyl alcohol) by using a strong magnetic field to obtain a unidirectional reinforced nanocomposite, and interestingly the results showed that the dynamic modulus of the nanocomposite was higher in the aligned direction compared with the transverse direction.[182]

Aqueous suspensions of CNs extracted from ramie fibers and tunicate have been allowed to dry under an AC electric field and have showed a high degree of orientation along the field vector in the films.[183] Colloidal suspensions of CNs from ramie fibers in cyclohexane have been also oriented in an AC electric field[184] as revealed by TEM and electron diffraction. Moreover, these suspensions demonstrated a birefringence when observed under polarized light with cross nicols whose magnitude could be increased with increasing field strength. They also displayed interference Newton colors, similar to those obtained for thin films of thermotropic liquid crystals, an interference pattern that reached a saturation plateau at ca. 2 kV/cm. This spectacular result was obtained at concentrations of CNs below the isotropic/nematic transition, which excluded any cooperative effect between the electric field and a possible anisotropic phase.[184]

5.4. Self-Assembly and -Organization of CNs in Thin Solid Films

Revol et al.[167,185] have taken advantage of the ability of suspensions of CNs to engage in lyotropic chiral nematic ordering to give rise to iridescent solid cellulosic films with unique and tunable optical properties by simply controlling the evaporation of suspending water on a flat surface. The liquid crystalline order obtained from these suspensions was preserved in solid films and the chiral nematic pitch in the dried films was on the same length scale as the wavelength

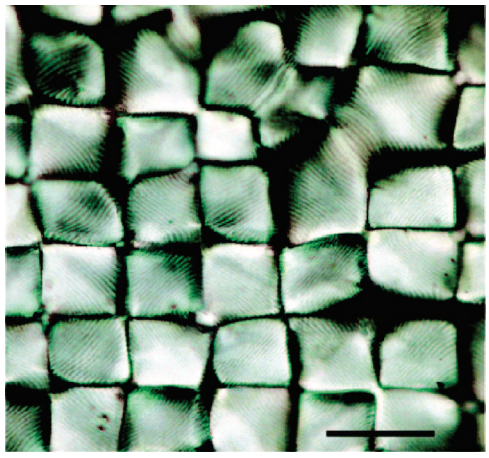

Figure 15. Square lattice in a solid film of cellulose nanocrystals between crossed polarizers. Scale bar 40 μm. Reprinted with permission from ref 186. Copyright 2005 American Chemical Society.

of visible light. This unique system was described as an interference device having the capacity to reflect circularly polarized light over a specific wavelength range. Because the wavelength of reflected light determines its spectral or intrinsic color, the perceived color of the film depends on the pitch of the cholesteric order and the angle of incidence of the light. The microstructure of such films is very sensitive to the drying conditions. Moreover, the perceived color of the reflected polarized light is "tunable" because the final pitch can be varied depending on processing variables such as the aspect ratio of CNs and the electrolyte content. Films that are prepared at ambient conditions generally show a polydomain (polymorphic) structure with the helical axes of different chiral nematic domains pointing in different directions. In fact, Roman and Gray[186,187] reported for the first time compelling evidence that a parabolic focal conic (PFC) structure (a symmetrical form of focal conic defects in which the line defects from a pair of perpendicular, antiparallel, and confocal parabolas) was trapped in these self-assembled solid films (see Figure 15).

Finally, it has been shown that a magnetic field during drying increased the size of the chiral nematic domains and affected the orientation of the helical axis with respect to the plane of the film.[179]

6. Applications of Cellulose Nanocrystals in Nanocomposite Materials

Since the first publication related to the use of CNs as reinforcing fillers in poly(styrene-*co*-butyl acrylate) (poly(S-*co*-BuA))-based nanocomposites by Favier et al.,[68] CNs have attracted a great deal of interest in the nanocomposites field due to their appealing intrinsic properties such as nanoscale dimensions, high surface area, unique morphology, low density (which is estimated to be 1.61 g/cm^3[188] for pure crystalline cellulose Iβ), and mechanical strength. In addition, they are easily (chemically) modified, readily available, renewable, and biodegradable. CNs have been incorporated into a wide range of polymer matrices, including polysiloxanes,[151] polysulfonates,[189] poly(caprolactone),[81,87,190] styrene−butyl acrylate latex,[191] poly(oxyethylene),[192−195] poly(styrene-*co*-butyl acrylate) (poly(S-*co*-BuA)),[68] cellulose acetate butyrate,[104,196] carboxymethyl cellulose,[197] poly(vinyl alcohol),[198] poly(vinyl acetate),[82,97] poly(ethylene−vinyl acetate) (EVA),[199] epoxides,[70] polyethylene,[131] polypropylene,[136] poly(vinyl chloride),[200−203] polyurethane,[204] and water-borne polyurethane.[98] Their incorporation into biopolymers, such as starch-based polymers,[69,89,90,205−208] soy protein,[209] chitosan,[130] or regenerated cellulose,[210] and biopolymer-like poly(lactic acid),[137,211−213] poly(hydroxyoctanoate),[214,215] and polyhydroxybutyrates[216] have also been reported.

6.1. Nanocomposite Processing

Processing techniques have an important impact on the final properties of the composites. The techniques that are adopted should take into consideration the intrinsic properties of CNs, their interfacial characteristics (modified or not), the nature of the polymeric matrix (solubility, dispersibility, and degradation), and the desired final properties such as geometrical shape.

6.1.1. Casting-Evaporation Processing

Casting evaporation has been the main technique to transfer cellulose whiskers from an aqueous dispersion into an organic polymer matrix. Nanocomposite films are formed via solution casting, that is, simply allowing the solvent to evaporate. Good dispersibility of the CNs in the polymer matrix, as well as in the processing solvent, is a prerequisite to create polymer/whisker nanocomposites that display a significant mechanical reinforcement. CNs without surface modification have intrinsically strong interactions and have been reported as notoriously difficult to disperse. Moreover, this issue is exacerbated when the CN dispersions are dried before nanocomposite processing, which generally implies that drying and redispersion of CNs without aggregation is challenging.

Due to the hydrophilic character of CNs, the simplest polymer systems that incorporate CNs are water-based. Never-dried aqueous dispersions of CNs are simply mixed with aqueous polymer solutions or dispersions. However, these systems suffer from limited utility and are only appropriate for water-soluble or dispersible polymers such as latexes. The combination of aqueous solutions of polymers (subject to moderately strong hydrogen bonding, in miscible cosolvents such as THF) with aqueous CN suspensions has been reported.[217] The use of polar solvents, most commonly *N*,*N*-dimethylformamide (DMF), with CNs with no surface modification has been explored.[218] Solvents nonmiscible with water and with low polarity, such toluene, have also been widely used. However, a drawback is that the process requires solvent exchange steps. Owing to the fact that acetone is miscible with water; it usually serves as carrier to transfer CNs from water to organic solvents. Freeze-drying and redispersion of CNs from tunicate in toluene were used to integrate these fillers into atactic polypropylene, but strong aggregation occurred.[153] However, when formic acid was used to redisperse dried CNs, very satisfactory dispersions were achieved.[219] Freeze-dried CNs were successfully redispersed in dipolar aprotic solvents, such DMSO and DMF, containing small amounts of water (0.1%), and it has been possible to obtain films of these suspensions by the casting-evaporation technique.[220] More recently van den Berg et al.[221] investigated the factors limiting the dispersibility of CNs extracted from tunicate via hydrochloric or sulfuric acid hydrolyses in a series of polar protic and aprotic organic solvents. HCl-generated CNs, which typically have a pronounced tendency to aggregate, did not disperse in polar aprotic solvents after being dried. Only protic solvents such

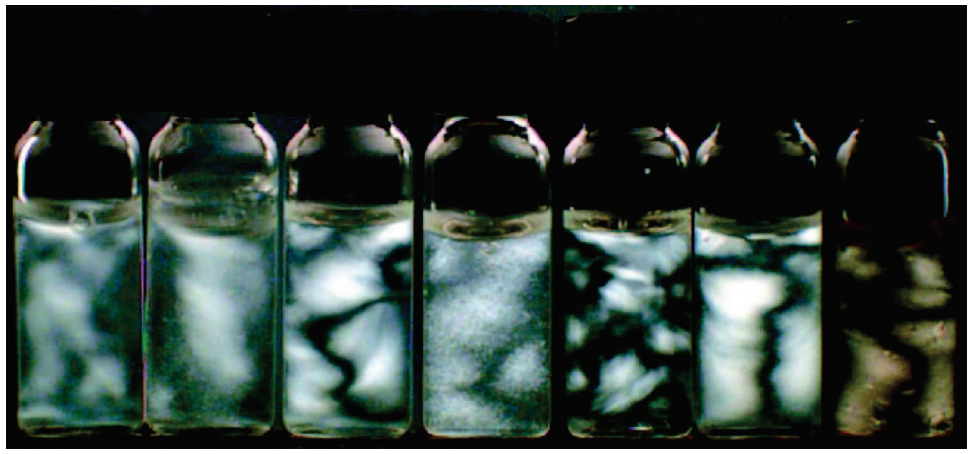

Figure 16. Photographs of 5.0 mg/mL dispersions of H_2SO_4-generated CNs viewed through cross polarizers: from left to right, as-prepared in water, freeze-dried, freeze-dried and redispersed in water, DMF, DMSO, *N*-methyl pyrrolidone, formic acid, and *m*-cresol. Reprinted with permission from ref 219. Copyright 2007 American Chemical Society.

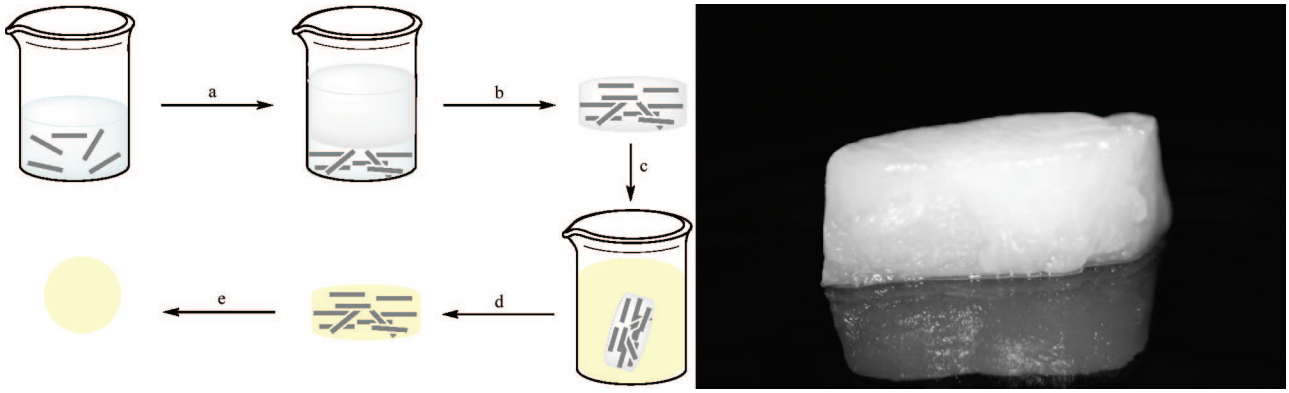

Figure 17. (left) Schematic representation of the template approach to obtain well-dispersed polymer/CN composites: (a) a nonsolvent is added to a dispersion of CNs in the absence of any polymer, (b) solvent exchange promotes the self-assembly of a gel of CNs, (c) the gelled CNs scaffold is interpenetrated with a polymer by immersion in a polymer solution, before the nanocomposite is (d) dried and (e) compacted. (right) The obtained gel after completing step b above Reprinted with permission from ref 101. Copyright 2009 American Chemical Society.

as formic acid and *m*-cresol were shown to effectively disrupt the hydrogen bonds in aggregated CNs, dispersing both types of CNs generated from hydrochloric or sulfuric acid hydrolyses (Figure 16).

Another approach already considered in this review to change interactions of CNs is via surface modifications. Such approach can break the percolating hydrogen-bonded network and affect the macroscopic mechanical properties of the resulting nanocomposite. Chemical modifications (discussed above) have been explored to improve dispersibility of CNs in wide range of organic solvents, from medium to low polarity. This approach also allows manipulation of dried CNs because it facilitates freeze-drying and redispersion.

6.1.2. Sol−Gel Processing

Capadona et al. have recently reported a versatile processing approach consisting of forming a three-dimensional template through self-assembly of well individualized CNs and then filling the template with a polymer of choice.[222−224] The first step (Figure 17 left, a and b) is the formation of a CN template through a sol/gel process involving the formation of a homogeneous aqueous whisker dispersion that is followed by gelation through solvent exchange with a water-miscible solvent (routinely acetone). In the second step (Figure 17 left, d and e), the CN template is filled with a matrix polymer by immersing the gel into a polymer solution (Figure 17). It should be noted that the polymer solvent must be miscible with the gel solvent and *de rigueur* not redisperse the CNs.

6.1.3. Other Processing Methods

The use of twin extrusion as a processing method to prepare CN-based nanocomposites has been attempted.[225] The process consists of pumping an aqueous dispersion of CNs coated with surfactant[226] or poly(vinyl alcohol)[211] into a melt polymer (i.e., poly(lactic acid), PLA) during extrusion. However, such systems have unfortunately shown a lack of compatibility. Starch and CN nanocomposites were processed by extrusion.[227] Moreover, the extrusion of modified CNs with long chained molecules seemed to be much easier and could be processed in solvent free conditions, especially when the grafted chains can melt at the processing temperature. An example has been reported recently where fatty acid-grafted CNs were successfully extruded with low-density polyethylene.[131] PCL-grafted CNs with long chains of PCL have shown good thermoformability when subjected to compression and injection.[156]

Electrostatic fiber spinning or electrospinning, a versatile method to manufacture fibers with diameters ranging from several micrometers down to 100 nm or less through the action of electrostatic forces, has emerged as an alternative processing method for CNs in polymer matrices. However,

as observed in the casting-evaporation technique, the dispersion of CNs can be challenging. Electrospun CNs in water-soluble polymers such as PEO[228] and PVA[229,230] by using water as solvent have been reported to result in fibers with diameters in the nanoscale range. Another technique to produce CN electrospun arrays has explored the avenue of using an indirect, sequestered "core-in-shell" electrospinning approach in which an aqueous dispersion of sulfated CNs constitutes the discrete "core" component surrounded by a cellulose "shell".[231] The various concurrent phenomena taking place during spinning, especially when loading the polymer suspension with CNs, make it difficult to control and to draw a clear-cut correlation between operational conditions and the properties of the produced micro- or nanofibers. Indeed, processing parameters such as the voltage and distance between the spinning tip and the collector, the properties (conductivity, viscosity, density, surface tension, etc.) of the spinning solution, and its flow rate can drastically affect the outcome of the spinning process.

There are various ways to electrospin polymer solutions containing CNs in organic media: several successful ones that have been reported include surfactant-coating[139] and polymer grafting[230,232] to disperse CNs in polystyrene dissolved in THF and polycaprolactone in DMF−dichloromethane. The use of polar solvents, such as DMF, has also been studied in the case of electrospinning PLA.[233]

Layer-by-layer deposition technique was also reported to produce CN-based multilayer composites.[234,235]

6.2. Mechanical Properties of CN-Based Composites

The nanoscale dimensions and extremely attractive mechanical properties of CNs make them ideal candidates to improve the mechanical properties of a targeted host material. In fact, the axial Young's modulus of a CN is theoretically stronger than steel and similar to that of Kevlar. For CNs, the theoretical value of Young's modulus for the native cellulose perfect crystal has been estimated to be 167.5 GPa.[236] Recently, the Raman spectroscopy technique was utilized to measure the elastic modulus of native cellulose crystals from tunicate and cotton to yield values of 143 GPa[237] and 105 GPa,[238] respectively.

Favier et al. reported for the first time, the reinforcing effect of CNs extracted from tunicate for reinforcing poly(S-co-BuA).[67,68] They demonstrated a spectacular improvement in the storage modulus, as measured by dynamic mechanical analysis, above the glass−rubber transition temperature range, even at low loading of CNs (see Figure 18).

It was demonstrated that the effect of CNs on the nanocomposite mechanical properties exceeded conventional predictions from traditional classical models applied to filler-reinforced nanocomposites, for example, as would be otherwise evident from the Halpin−Kardos model.[239] This effect was explained, in part, by the formation of a rigid percolating filler network that was cemented together by hydrogen bonds.[240] The presence of such a network was later confirmed by electrical measurements performed on nanocomposites containing CNs that were coated with conductive polypyrrole.[241]

Percolation is a statistical geometrical model that can be applied to any random multiphase material involving components that are able to commingle.[242] By variation of the number of connections, this approach allows for a transition

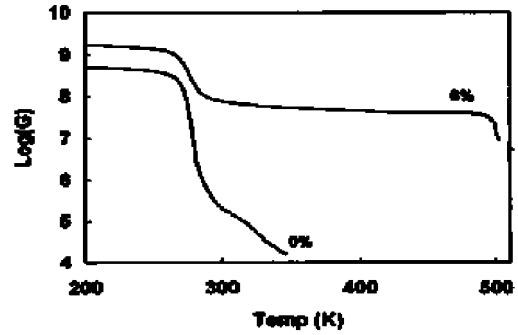

Figure 18. Logarithm of storage shear modulus versus temperature for poly(S-co-BuA) nanocomposite reinforced by 6% weight fraction of tunicate cellulose nanocrystals. Reprinted with permission from ref 68. Copyright 1995 American Chemical Society.

from a disconnected set of objects to an infinite connected state. The percolation threshold is defined as the critical volume fraction separating these two states. The volume threshold depends upon a number of variables, primarily the shape of the particles (size[243] and aspect ratio[244]), their orientation,[245] and the interparticle interactions.[246]

Therefore, to study the reinforcing effect of CNs, a model must be invoked involving the three different phases in a typical composite: the matrix, the filler percolating network, and the nonpercolating filler. By extending the phenomenological series-parallel model of Takayanagi et al.,[247] Ouali et al.[248] suggested a construct in which the topological arrangement of the fillers and their interactions were taken into account. In this approach, the elastic tensile modulus G' of the composite was given by the following equation:

$$G' = \frac{(1 - 2\psi + \psi X_r)G'_s G'_r + (1 - X_r)\psi G'^2_r}{(1 - X_r)G'_r + (X_r - \psi)G'_s}$$

The subscripts s and r refer to the soft phase (polymer) and rigid phase (CNs), respectively. The adjustable parameter, ψ, corresponds to the volume fraction of the percolating rigid phase, with b being the critical percolation exponent. ψ can be written as

$$\psi = 0 \quad \text{for} \quad X_r < X_c$$
$$\psi = X_r\left(\frac{X_r - X_c}{1 - X_c}\right)^b \quad \text{for} \quad X_r > X_c$$

in which $b = 0.4$ for a three-dimensional network.[242] X_r is the volume fraction of CNs, and X_c is the critical percolation volume fraction (percolation threshold) required to achieve the geometrical percolation. To calculate X_c, Favier et al.[249] developed the following relation by using a statistical percolation theory for cylindrically shaped particles, taking into account their aspect ratio: $X_c = 0.7/A$ where A is the aspect ratio of CNs, which is the ratio between their length and width (L/w).

At temperatures high enough to assume that the polymeric matrix has zero stiffness ($G'_s \approx 0$), the calculated stiffness of the composite is simply the result of the percolating filler network and the volume fraction of percolating filler phase:

$$G'_c = \psi G'_r$$

This model gave satisfactory results in the case of Favier's system, and recently excellent correlations have been obtained between the predicted percolation model values and

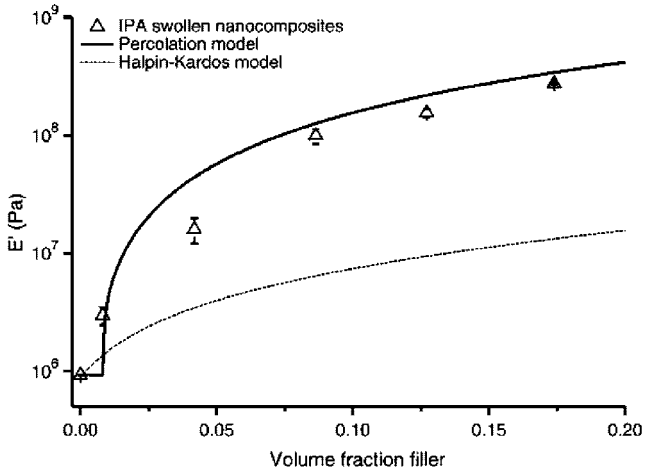

Figure 19. Experimental and predicted (percolation and Halpin−Kardos model) values of the tensile storage moduli (E') of EO-EPI/CN nanocomposites as a function of volume fraction of cellulose nanocrystals. From ref 224, reprinted with permission from AAAS.

the experimental data for nanocomposites as shown in Figure 19.[224] Detailed information about this percolation phenomenon in CN-based composites has been reported by Aziz Samir et al.[250]

The mechanical properties of composites are mainly affected by factors that ensure or interfere with the formation of the percolated network such the dimensions of CNs and their interfacial interactions (between them or with the host matrix). This percolation network can therefore be modified by altering the surface chemistry of the nanoparticle. The processing method has been also reported to impact the mechanical properties.

6.2.1. Morphology and Dimensions of CNs

Because the geometrical aspect ratio of CNs determines the percolation threshold value, the dimensions have an important influence on the mechanical properties. Obviously, CNs with high aspect ratio give the best reinforcing effect because lower amounts are needed to achieve the percolation. But this latter assertion depends on the source of cellulose fibers and the conditions of hydrolysis during CN preparation as described previously (*vide infra*).

6.2.2. Processing Method

The conditions, such the processing rate and the viscosity of the system, can have an effect on the ability of the percolating structure to be cemented or to withstand imposed stresses. The sol−gel processing method seems to give the highest mechanical performance because the percolation network is formed and strong interactions are created at the CN contact points before the addition of the polymer solution. The casting-evaporation technique also gives satisfactory results in terms of mechanical performance. During such slow processing methods, CNs have adequate time to interconnect and form a percolation network. This ability to connect is also related to the Brownian motion and the rearrangement of the CNs that occurs in the suspension when the viscosity of the system remains low until the end of the process. In contrast, high polymer melt viscosity that occurs during hot pressing or extrusion processes strongly limits random movement and consequently hinders the interconnection between CNs. Possible alignments of CNs owing to induced shear stresses during extrusion or molding may also affect the network formation. Hajji et al.[251] studied the effect of the processing method on the mechanical properties of CN-based nanocomposites and classified them in ascending order of their reinforcement efficiency: extrusion < hot pressing < evaporation.

6.2.3. Interfacial Interactions

The origin of the enhancement of the mechanical properties is the rigid network that is formed among the CNs joined by hydrogen bonds. Any factor, such as the nature of the polymer matrix and the surface energy of the CNs, will influence the formation of a network and will have a great impact on the mechanical performance of the resulting composites. Compromised interactions among all competitions that may occur such as matrix/CN and CN/CN interactions have to be reached to achieve optimal mechanical properties.[252] CNs are usually extricated from the matrix if very poor compatibility occurs between them resulting in a disastrous decline in the mechanical properties. Surprisingly a very good compatibility between CNs and the host polymer has a propensity to decrease the elastic modulus of the composite, typically when nanocomposites are processed via a casting method. This behavior is most likely due the restricted mobility of CNs, which tend to strongly interact with the polymer chains rather than extending to each other to interconnect and form the network. An example of this behavior has been clearly evidenced in the case of glycerol-plasticized starch reinforced with CNs extracted from cottonseed linters.[207] However, into polymer matrices this does not seem to happen when the percolation network is formed before the addition of the polymer solution by using a sol−gel processing method. On the other hand, strong matrix/CN interactions seem to enhance the nonlinear mechanical properties especially the ultimate strain when CNs are chemically modified with long-chain molecules such as surfactants,[135,153] *N*-octadecyl isocyanate,[92] fatty acids,[131] or polymer chains.[87,98] In fact when CNs were grafted with high molecular weight PCL, for example, and then incorporated in a PCL matrix, the final nanocomposite showed a lower modulus, but significantly higher strain at break compared with the control filled with unmodified CNs.[87] This behavior clearly reflected the restricted CN/CN interactions that drop the modulus and the high CN/matrix compatibilization resulting from the formation of a percolating network held by chain entanglements and possible cocrystallization between the grafted chains and the matrix. Similarly, Cao et al.[98] have reported that chain entanglements and cocrystallization occurred in nanocomposites based on a completely amorphous polymer, that is, polyurethane reinforced with CNs that have been grafted with the same polymer in a one-pot process.

6.3. Thermal Properties of CN-Based Composites

Surprisingly, most studies in this field report that the addition of CNs into polymers matrices does not seem to affect the glass−rubber transition temperature, T_g, regardless of the nature of the host polymer, the origin of the CNs, or the processing conditions.[250,253] This observation seems to be in conflict with the fact that CNs have a high specific area. There are a few cases reported in the literature where the addition of CNs as filler in nanocomposite materials affected the T_g. This effect, shown especially in moisture-

sensitive systems,[97] was related to the plasticization effect of water and was also linked to the strong interaction between CNs and the matrix.

In the case of semicrystalline polymers, it was reported that the addition of unmodified CNs has no influence on the melting temperature (T_m) of the nanocomposites, as has been shown in the case of plasticized starch,[107,254] poly(ethylene oxide),[195,255] cellulose acetate butyrate,[104,150] polycaprolactone-reinforced polymers,[81,87] etc. However, when chemically modified CNs were used in nanocomposites, a change of T_m was observed. Strong interactions between chemically modified CNs and matrices have been reported to be the origin of this T_m change. Moreover, CNs can act as nucleating agents in semicrystalline polymers, which significantly increases the crystallinity of the ensuing nanocomposites.[87,135] This effect is mainly governed by the CN−matrix compatibility, which depends on surface chemical considerations. A transcrystallization phenomenon has been reported in CN-reinforced nanocomposites.[256] Recently Cao et al.[98] investigated the use of chemically modified CNs (grafted with the same polymer as the matrix) as a filler in completely amorphous polyurethane. They observed partial crystallization and transformation of the nanocomposite material from an elastomer-like to a thermoplastic-like material. This unusual behavior is related to the chain entanglements that take place between the grafted chains and those from the polymer matrix.

7. Conclusions and Outlook

The breadth, diversity, and richness of research that has been inspired over the past few years by cellulose nanocrystals has been astonishing, but not entirely unexpected in the current biomass and bioenergy conscious climate. This review has attempted to provide a broad vista of the intriguing scientific and engineering discoveries and advancements that have been accomplished up to the present in hopes of stimulating increased interest in their intrinsically appealing characteristics. These remarkable nanoscopic entities lend themselves to a plethora of chemical transformations and have thus been manipulated to provide a rich suite of new materials and platforms for further transformations. For example, their polyol nature allows them to anchor a host of non-native chemical functionalities that can modulate their hydrophilic/lipophilic balance, change their aggregation and hierarchical organization, and impart optical, electrical, or magnetic tunability. The overall gamut of material applications for cellulose nanocrystals is virtually limitless; in addition, the possibility of controlling their biosynthetic pathways (e.g., to control crystallinity) opens up new windows to encouraging their use as a facile energy resource for bioenergy technologies. Currently, the field is in its infancy and provides the chemical, biological, physical, and engineering communities a virtual cornucopia of opportunities for new advancements and discoveries.

8. Acknowledgments

The authors wish to dedicate this review to the memory of Dr. Jean-François Revol who was instrumental in the development and use of cellulose nanocrystal suspensions. We also gratefully acknowledge financial support from the Southeastern Sun Grant Center and U.S. Department of Transportation (Grant No. 101571) and National Research Initiative of the USDA Cooperative State Research, Education and Extension Service, Grant Nos. 2007-35504-18290 and 2008-35504-19203. Finally, we are grateful for support from USDA Grant No. 2006-38411-17035 (Higher Education Challenge) that made portions of this work possible.

9. References

(1) French, A. D.; Bertoniere, N. R.; Brown, R. M.; Chanzy, H.; Gray, D.; Hattori, K.; Glasser, W. In *Kirk-Othmer Encyclopedia of Chemical Technology* 5th ed.; Seidel, A., Ed.; John Wiley & Sons, Inc.: New York, 2004; Vol. 5.
(2) Payen, A. *Compt. Rend.* **1838**, *7*, 1052.
(3) Atalla, R. H. *Compr. Nat. Prod. Chem.* **1999**, *3*, 529.
(4) Atalla, R. H. *Lenzinger Ber.* **2000**, *79*, 5.
(5) Atalla, R. H.; Brady, J. W.; Matthews, J. F.; Ding, S.-Y.; Himmel, M. E. *Biomass Recalcitrance* **2008**, 188.
(6) Fengel, D.; Wegener, G. *Wood, Chemistry, Ultrastucture, Reactions*; Walter de Gruyter: New York, 1983.
(7) Hon, D. N.-S.; Shiraishi, N. *Wood and Cellulosic Chemistry*; Marcel Dekker, Inc.: New York, 1991.
(8) Marchessault, R. H.; Sundararajan, P. R. In *The Polysaccharides*; Aspinall, G. O., Ed.; Academic Press: New York, 1983.
(9) O'Sullivan, A. C. *Cellulose* **1997**, *4*, 173.
(10) Sarko, A. In *Wood and Cellulosics: Industrial Utilisation, Biotechnology, Structure, and Properties*; Kennedy, J. F., Ed.; Ellis Horwood: Chichester, U.K., 1987.
(11) Salmon, S.; Hudson, S. M. *Polym. Rev.* **1997**, *37*, 199.
(12) Klemm, D.; Heublein, B.; Fink, H.-P.; Bohn, A. *Angew. Chem., Int. Ed.* **2005**, *44*, 3358.
(13) Preston, R. D. In *Cellulose: Structure, Modification and Hydrolysis*; Young, R. A., Rowell, R. M., Eds.; John Wiley and Sons: New York, 1986.
(14) Brown, R. M. J. *J. Macromol. Sci., Part A: Pure Appl. Chem.* **1996**, *A33*, 1345.
(15) Williamson, R. E.; Burn, J. E.; Hocart, C. H. *Trends Plant Sci.* **2002**, *7*, 461.
(16) Haigler, C. H. In *Biosynthesis and Biodegradation of Cellulose*; Haigler, C. H., Weimer, P., Eds.; Marcel Dekker: New York, 1991.
(17) Vincent, J. F. V. *Mater. Today* **2002**, *5*, 28.
(18) Brown, R. M. J. *J. Polym. Sci., Part A: Polym. Chem.* **2004**, *42*, 487.
(19) Rowland, S. P.; Roberts, E. J. *J. Polym. Sci., Part A: Polym. Chem.* **1972**, *10*, 2447.
(20) Atalla, R. H. *Struct., Funct., Biosynth. Plant Cell Walls, Proc. Annu. Symp. Bot., 7th* **1984**, 381.
(21) Atalla, R. H.; VanderHart, D. L. *Science* **1984**, *223*, 283.
(22) VanderHart, D. L.; Atalla, R. H. *Macromolecules* **1984**, *17*, 1465.
(23) Atalla, R. H.; VanderHart, D. L. *Solid State Nucl. Magn. Reson.* **1999**, *15*, 1.
(24) Nishiyama, Y.; Sugiyama, J.; Chanzy, H.; Langan, P. *J. Am. Chem. Soc.* **2003**, *125*, 14300.
(25) Nishiyama, Y.; Langan, P.; Chanzy, H. *J. Am. Chem. Soc.* **2002**, *124*, 9074.
(26) Sugiyama, J.; Okano, T.; Yamamoto, H.; Horii, F. *Macromolecules* **1990**, *23*, 3196.
(27) Wada, M.; Nishiyama, Y.; Chanzy, H.; Forsyth, T.; Langan, P. *Adv. X-Ray Anal.* **2008**, *51*, 138.
(28) Jarvis, M. C. *Carbohydr. Res.* **2000**, *325*, 150.
(29) Liang, C. Y.; Marchessault, R. H. *J. Polym. Sci.* **1959**, *37*, 385.
(30) Honjo, G.; Watanabe, M. *Nature* **1958**, *181*, 326.
(31) Nishiyama, Y.; Chanzy, H.; Wada, M.; Sugiyama, J.; Mazeau, K.; Forsyth, T.; Riekel, C.; Mueller, M.; Rasmussen, B.; Langan, P. *Adv. X-Ray Anal.* **2002**, *45*, 385.
(32) Sturcova, A.; His, I.; Apperley, D. C.; Sugiyama, J.; Jarvis, M. C. *Biomacromolecules* **2004**, *5*, 1333.
(33) Schweizer, E. J. *J. Prakt. Chem.* **1857**, *72*, 109.
(34) Jayme, G. In *Cellulose and Cellulose Derivatives*; Bikales, N. M., Segal, L., Eds.; Wiley: New York, 1971.
(35) Hudson, S. M.; Cuculo, J. A. *J. Polym. Sci., Polym. Chem. Ed.* **1980**, *18*, 3469.
(36) Hattori, K.; Cuculo, J. A.; Hudson, S. M. *J. Polym. Sci., Part A: Polym. Chem.* **2002**, *40*, 601.
(37) Dawsey, T. R.; McCormick, C. L. *J. Macromol. Sci., Rev. Macromol. Chem. Phys.* **1990**, *C30*, 405.
(38) McCormick, C. L.; Shen, T. C. *Org. Coat. Plast. Chem.* **1981**, *45*, 335.
(39) Chanzy, H.; Paillet, M.; Peguy, A. *Polym. Commun.* **1986**, *27*, 171.
(40) Katrib, F. A.; Chambat, G.; Joseleau, J. P. *Cellul. Chem. Technol.* **1988**, *22*, 305.
(41) Maia, E.; Peguy, A.; Perez, S. *Acta Crystallogr., Sect. B* **1981**, *B37*, 1858.

(42) Parnell, E. A. *The life and labours of John Mercer*; Longmans, Green & Co.: London, 1886.
(43) Chedin, J.; Marsaudon, A. *Chim. Ind. (Paris)* **1954**, *71*, 55.
(44) Kuga, S.; Takagi, S.; Brown, R. M., Jr. *Polymer* **1993**, *34*, 3293.
(45) Langan, P.; Nishiyama, Y.; Chanzy, H. *Biomacromolecules* **2001**, *2*, 410.
(46) Langan, P.; Sukumar, N.; Nishiyama, Y.; Chanzy, H. *Cellulose* **2005**, *12*, 551.
(47) Langan, P.; Nishiyama, Y.; Chanzy, H. *J. Am. Chem. Soc.* **1999**, *121*, 9940.
(48) Sturcova, A.; His, I.; Wess, T. J.; Cameron, G.; Jarvis, M. C. *Biomacromolecules* **2003**, *4*, 1589.
(49) Whitmore, R. E.; Atalla, R. H. *Int. J. Biol. Macromol.* **1985**, *7*, 182.
(50) Okano, T.; Kim, N. H.; Sugiyama, J. *Cellulose* **1990**, 93.
(51) Mann, J.; Marrinan, H. J. *Chem. Ind.* **1953**, 1092.
(52) Wada, M.; Chanzy, H.; Nishiyama, Y.; Langan, P. *Macromolecules* **2004**, *37*, 8548.
(53) Wada, M.; Heux, L.; Nishiyama, Y.; Langan, P. *Biomacromolecules* **2009**, *10*, 302.
(54) Gardiner, E. S.; Sarko, A. *J. Appl. Polym. Sci.: Appl. Polym. Symp.* **1983**, *37*, 303.
(55) Gardiner, E. S.; Sarko, A. *Can. J. Chem.* **1985**, *63*, 173.
(56) Chanzy, H.; Imada, K.; Mollard, A.; Vuong, R.; Barnoud, F. *Protoplasma* **1979**, *100*, 303.
(57) Helbert, W.; Sugiyama, J.; Ishihara, M.; Yamanaka, S. *J. Biotechnol.* **1997**, *57*, 29.
(58) Rånby, B. G. *Acta Chem. Scand.* **1949**, *3*, 649.
(59) Rånby, B. G. *Discuss. Faraday Soc.* **1951**, *11*, 158.
(60) Rånby, B. G.; Ribi, E. *Experimentia* **1950**, *6*, 12.
(61) Nickerson, R. F.; Habrle, J. A. *Ind. Eng. Chem.* **1947**, *39*, 1507.
(62) Mukherjee, S. M.; Sikorski, J.; Woods, H. J. *J. Text. Inst.* **1952**, *43*, T196.
(63) Mukherjee, S. M.; Woods, H. J. *Biochim. Biophys. Acta* **1953**, *10*, 499.
(64) Battista, O. A. *Ind. Eng. Chem.* **1950**, *42*, 502.
(65) Battista, O. A.; Coppick, S.; Howsmon, J. A.; Morehead, F. F.; Sisson, W. A. *Ind. Eng. Chem.* **1956**, *48*, 333.
(66) Marchessault, R. H.; Morehead, F. F.; Walter, N. M. *Nature* **1959**, *184*, 632.
(67) Favier, V.; Canova, G. R.; Cavaille, J. Y.; Chanzy, H.; Dufresne, A.; Gauthier, C. *Polym. Adv. Technol.* **1995**, *6*, 351.
(68) Favier, V.; Chanzy, H.; Cavaille, J. Y. *Macromolecules* **1995**, *28*, 6365.
(69) Angles, M. N.; Dufresne, A. *Macromolecules* **2001**, *34*, 2921.
(70) Ruiz, M. M.; Cavaille, J. Y.; Dufresne, A.; Gerard, J. F.; Graillat, C. *Compos. Interfaces* **2000**, *7*, 117.
(71) Sharples, A. *Trans. Faraday Soc.* **1958**, *54*, 913.
(72) Yachi, T.; Hayashi, J.; Takai, M.; Shimizu, Y. *J. Appl. Polym. Sci.: Appl. Polym. Symp.* **1983**, *37*, 325.
(73) Håkansson, H.; Ahlgren, P. *Cellulose* **2005**, *12*, 177.
(74) Martin, C. *J. Polym. Sci., Part C: Polym. Lett.* **1971**, *36*, 343.
(75) Martin, M. Y. C. *J. Polym. Sci.: Polym. Chem. Ed.* **1974**, *12*, 1349.
(76) Schurz, J.; John, K. *Cellul. Chem. Technol.* **1975**, *9*, 493.
(77) Nishiyama, Y.; Kim, U. J.; Kim, D. Y.; Katsumata, K. S.; May, R. P.; Langan, P. *Biomacromolecules* **2003**, *4*, 1013.
(78) Kai, A. *Sen-i Gakkaishi* **1976**, *32*, T326.
(79) Elazzouzi-Hafraoui, S.; Nishiyama, Y.; Putaux, J.-L.; Heux, L.; Dubreuil, F.; Rochas, C. *Biomacromolecules* **2008**, *9*, 57.
(80) Roman, M.; Winter, W. T. *Biomacromolecules* **2004**, *5*, 1671.
(81) Habibi, Y.; Goffin, A.-L.; Schiltz, N.; Duquesne, E.; Dubois, P.; Dufresne, A. *J. Mater. Chem.* **2008**, *18*, 5002.
(82) Garcia de Rodriguez, N. L.; Thielemans, W.; Dufresne, A. *Cellulose* **2006**, *13*, 261.
(83) Bai, W.; Holbery, J.; Li, K. *Cellulose* **2009**, *16*, 455.
(84) de Souza Lima, M. M.; Borsali, R. *Langmuir* **2002**, *18*, 992.
(85) Dong, X. M.; Revol, J.-F.; Gray, D. G. *Cellulose* **1998**, *5*, 19.
(86) Araki, J.; Wada, M.; Kuga, S.; Okano, T. *Langmuir* **2000**, *16*, 2413.
(87) Habibi, Y.; Dufresne, A. *Biomacromolecules* **2008**, *9*, 1974.
(88) Habibi, Y.; Foulon, L.; Aguié-Béghin, V.; Molinari, M.; Douillard, R. *J. Colloid Interface Sci.* **2007**, *316*, 388.
(89) Cao, X.; Chen, Y.; Chang, P. R.; Stumborg, M.; Huneault, M. A. *J. Appl. Polym. Sci.* **2008**, *109*, 3804.
(90) Cao, X.; Chen, Y.; Chang, P. R.; Muir, A. D.; Falk, G. *eXPRESS Polym. Lett.* **2008**, *2*, 502.
(91) Cao, X.; Dong, H.; Li, C. M. *Biomacromolecules* **2007**, *8*, 899.
(92) Siqueira, G.; Bras, J.; Dufresne, A. *Biomacromolecules* **2009**, *10*, 425.
(93) Helbert, W.; Cavaille, J. Y.; Dufresne, A. *Polym. Compos.* **1996**, *17*, 604.
(94) Bendahou, A.; Habibi, Y.; Kaddami, H.; Dufresne, A. *J. Biobased Mater. Bioenergy* **2009**, *3*, 81.
(95) Araki, J.; Wada, M.; Kuga, S.; Okano, T. *J. Wood Sci.* **1999**, *45*, 258.
(96) Beck-Candanedo, S.; Roman, M.; Gray, D. G. *Biomacromolecules* **2005**, *6*, 1048.
(97) Roohani, M.; Habibi, Y.; Belgacem, N. M.; Ebrahim, G.; Karimi, A. N.; Dufresne, A. *Eur. Polym. J.* **2008**, *44*, 2489.
(98) Cao, X.; Habibi, Y.; Lucia, L. A. *J. Mater. Chem.* **2009**, *19*, 7137.
(99) Bondeson, D.; Mathew, A.; Oksman, K. *Cellulose* **2006**, *13*, 171.
(100) Pranger, L.; Tannenbaum, R. *Macromolecules* **2008**, *41*, 8682.
(101) Capadona, J. R.; Shanmuganathan, K.; Trittschuh, S.; Seidel, S.; Rowan, S. J.; Weder, C. *Biomacromolecules* **2009**, *10*, 712.
(102) Bondeson, D.; Kvien, I.; Oksman, K. In *Cellulose Nanocomposites: Processing, Characterization, and Properties*; Oksman, K., Sain, M., Eds.; ACS Symposium Series 938; American Chemical Society: Washington, DC, 2006.
(103) Azizi Samir, M. A. S.; Alloin, F.; Paillet, M.; Dufresne, A. *Macromolecules* **2004**, *37*, 4313.
(104) Grunnert, M.; Winter, W. T. *J. Polym. Environ.* **2002**, *10*, 27.
(105) Araki, J.; Kuga, S. *Langmuir* **2001**, *17*, 4493.
(106) Hirai, A.; Inui, O.; Horii, F.; Tsuji, M. *Langmuir* **2009**, *25*, 497.
(107) Angles, M. N.; Dufresne, A. *Macromolecules* **2000**, *33*, 8344.
(108) Koshizawa, T. *Kami Pa Gikyoshi* **1960**, *14*, 455.
(109) Okano, T.; Kuga, S.; Wada, M.; Araki, J.; Ikuina, J.; (Nisshin Oil Mills Ltd., Japan). JP 98/151052, 1999.
(110) Ono, H.; Matsui, T.; Miyamato, I.; (Asahi Kasei Kogyo Kabushiki Kaisha, Japan). WO 98/JP5462, 1999.
(111) Usuda, M.; Suzuki, O.; Nakano, J.; Migita, N. *Kogyo Kagaku Zasshi* **1967**, *70*, 349.
(112) Filpponen, I. Ph.D. Thesis, North Carolina State University, Raleigh, NC, 2009.
(113) Araki, J.; Wada, M.; Kuga, S.; Okano, T. *Colloids Surf., A* **1998**, *142*, 75.
(114) Revol, J. F.; Bradford, H.; Giasson, J.; Marchessault, R. H.; Gray, D. G. *Int. J. Biol. Macromol* **1992**, *14*, 170.
(115) Wang, N.; Ding, E.; Cheng, R. *Langmuir* **2008**, *24*, 5.
(116) Wang, N.; Ding, E.; Cheng, R. *Polymer* **2007**, *48*, 3486.
(117) Miller, A. F.; Donald, A. M. *Biomacromolecules* **2003**, *4*, 510.
(118) Terech, P.; Chazeau, L.; Cavaille, J. Y. *Macromolecules* **1999**, *32*, 1872.
(119) de Souza Lima, M. M.; Wong, J. T.; Paillet, M.; Borsali, R.; Pecora, R. *Langmuir* **2003**, *19*, 24.
(120) Hanley, S. J.; Giasson, J.; Revol, J. F.; Gray, D. G. *Polymer* **1992**, *33*, 4639.
(121) Hanley, S. J.; Revol, J.-F.; Godbout, L.; Gray, D. G. *Cellulose* **1997**, *4*, 209.
(122) Kvien, I.; Tanem, B. S.; Oksman, K. *Biomacromolecules* **2005**, *6*, 3160.
(123) Lahiji, R. R.; Reifenberger, R.; Raman, A.; Rudie, A.; Moon, R. J. *NSTI Nanotech, Nanotechnol. Conf. Trade Show, Tech. Proc.* **2008**, 704.
(124) Helbert, W.; Nishiyama, Y.; Okano, T.; Sugiyama, J. *J. Struct. Biol.* **1998**, *124*, 42.
(125) Revol, J. F. *Carbohydr. Polym.* **1982**, *2*, 123.
(126) Sassi, J.-F.; Chanzy, H. *Cellulose* **1995**, *2*, 111.
(127) Araki, J.; Wada, M.; Kuga, S. *Langmuir* **2001**, *17*, 21.
(128) Dong, X. M.; Kimura, T.; Revol, J.-F.; Gray, D. G. *Langmuir* **1996**, *12*, 2076.
(129) Heux, L.; Chauve, G.; Bonini, C. *Langmuir* **2000**, *16*, 8210.
(130) Li, Q.; Zhou, J.; Zhang, L. *J. Polym. Sci., Part B: Polym. Phys.* **2009**, *47*, 1069.
(131) Junior de Menezes, A.; Siqueira, G.; Curvelo, A. A. S.; Dufresne, A. *Polymer* **2009**, *50*, 4552.
(132) Kimura, F.; Kimura, T.; Tamura, M.; Hirai, A.; Ikuno, M.; Horii, F. *Langmuir* **2005**, *21*, 2034.
(133) Heux, L.; Bonini, C. International Patent WO 2000/077088, 2000.
(134) Bonini, C.; Heux, L.; Cavaille, J.-Y.; Lindner, P.; Dewhurst, C.; Terech, P. *Langmuir* **2002**, *18*, 3311.
(135) Ljungberg, N.; Cavaillé, J.-Y.; Heux, L. *Polymer* **2006**, *47*, 6285.
(136) Bonini, C. Ph.D. Thesis, Joseph Fourier University, Grenoble, France, 2000.
(137) Bondeson, D.; Oksman, K. *Compos. Interfaces* **2007**, *14*, 617.
(138) Kim, J.; Montero, G.; Habibi, Y.; Hinestroza, J. P.; Genzer, J.; Argyropoulos, D. S.; Rojas, O. J. *Polym. Eng. Sci.* **2009**, *49*, 2054.
(139) Rojas, O. J.; Montero, G. A.; Habibi, Y. *J. Appl. Polym. Sci.* **2009**, *113*, 927.
(140) Zhou, Q.; Brumer, H.; Teeri, T. T. *Macromolecules* **2009**, *42*, 5430.
(141) de Nooy, A. E. J.; Besemer, A. C.; van Bekkum, H. *Recl. Trav. Chim. Pays-Bas* **1994**, *113*, 165.
(142) Montanari, S.; Roumani, M.; Heux, L.; Vignon, M. R. *Macromolecules* **2005**, *38*, 1665.
(143) Habibi, Y.; Chanzy, H.; Vignon, M. R. *Cellulose* **2006**, *13*, 679.
(144) Hasani, M.; Cranston, E. D.; Westmana, G.; Gray, D. G. *Soft Matter* **2008**, *4*, 2238.
(145) Braun, B.; Dorgan, J. R. *Biomacromolecules* **2009**, *10*, 334.

(146) Sobkowicz, M. J.; Braun, B.; Dorgan, J. R. *Green Chem.* **2009**, *11*, 680.
(147) Yuan, H.; Nishiyama, Y.; Wada, M.; Kuga, S. *Biomacromolecules* **2006**, *7*, 696.
(148) Berlioz, S.; Molina-Boisseau, S.; Nishiyama, Y.; Heux, L. *Biomacromolecules* **2009**, *10*, 2144.
(149) Gousse, C.; Chanzy, H.; Excoffier, G.; Soubeyrand, L.; Fleury, E. *Polymer* **2002**, *43*, 2645.
(150) Roman, M.; Winter, W. T. In *Cellulose Nanocomposites: Processing, Characterization, and Properties*; Oksman, K., Sain, M., Eds.; ACS Symposium Series 938; American Chemical Society: Washington, DC, 2006.
(151) Grunnert, M.; Winter, W. T. *Polym. Mater. Sci. Eng.* **2000**, *82*, 232.
(152) Zhao, B.; Brittain, W. J. *Prog. Polym. Sci.* **2000**, *25*, 677.
(153) Ljungberg, N.; Bonini, C.; Bortolussi, F.; Boisson, C.; Heux, L.; Cavaille, J. Y. *Biomacromolecules* **2005**, *6*, 2732.
(154) Vignon, M.; Montanari, S.; Habibi, Y. (Centre National de la Recherche Scientifique CNRS, Fr.) FR 2003/5195, 2004.
(155) Mangalam, A. P.; Simonsen, J.; Benight, A. S. *Biomacromolecules* **2009**, *10*, 497.
(156) Chen, G.; Dufresne, A.; Huang, J.; Chang, P. R. *Macromol. Mater. Eng.* **2009**, *294*, 59.
(157) Lin, N.; Chen, G.; Huang, J.; Dufresne, A.; Chang, P. R. *J. Appl. Polym. Sci.* **2009**, *113*, 3417.
(158) Yi, J.; Xu, Q.; Zhang, X.; Zhang, H. *Polymer* **2008**, *49*, 4406.
(159) Morandi, G.; Heath, L.; Thielemans, W. *Langmuir* **2009**, *25*, 8280.
(160) Zoppe, J.; Habibi, Y.; Efimenko, K.; Genzer, J.; Rojas, O. J. *Abstr. Pap., ACS Natl. Meet.* **2009**, *237*, CELL-046.
(161) Zoppe, J.; Habibi, Y.; Rojas, O. J. *Abstr. Pap., ACS Natl. Meet.* **2008**, *235*, CELL-057.
(162) Mattoso, L. H. C.; Medeiros, E. S.; Baker, D. A.; Avloni, J.; Wood, D. F.; Orts, W. J. *J. Nanosci. Nanotechnol.* **2009**, *9*, 2917.
(163) Folda, T.; Hoffman, H.; Chanzy, H.; Smith, P. *Nat. Nanotechnol.* **1988**, *333*, 55.
(164) Oster, G. *J. Gen. Physiol.* **1950**, *33*, 445.
(165) Livolant, F.; Leforestier, A. *Prog. Polym. Sci.* **1996**, *21*, 1115.
(166) Revol, J.-F.; Marchessault, R. H. *Int. J. Biol. Macromol.* **1993**, *15*, 329.
(167) Revol, J.-F.; Godbout, J. D. L.; Gray, D. G. International Patent WO 95/21901, 1995.
(168) Roland, J. C.; Reis, D.; Vian, B.; Roy, S. *Biol. Cell.* **1989**, *67*, 209.
(169) Neville, A. C.; Gubb, D. C.; Crawford, R. M. *Protoplasma* **1976**, *90*, 307.
(170) Orts, W. J.; Godbout, L.; Marchessault, R. H.; Revol, J. F. *Macromolecules* **1998**, *31*, 5717.
(171) Onsager, L. *Ann. N.Y. Acad. Sci.* **1949**, *51*, 627.
(172) Stroobants, A.; Lekkerkerker, H. N. W.; Odijk, T. *Macromolecules* **1986**, *19*, 2232.
(173) Dong, X. M.; Gray, D. G. *Langmuir* **1997**, *13*, 2404.
(174) Beck-Candanedo, S.; Viet, D.; Gray, D. G. *Cellulose* **2006**, *13*, 629.
(175) Beck-Candanedo, S.; Viet, D.; Gray, D. G. *Langmuir* **2006**, *22*, 8690.
(176) Beck-Candanedo, S.; Viet, D.; Gray, D. G. *Macromolecules* **2007**, *40*, 3429.
(177) Elazzouzi-Hafraoui, S.; Putaux, J.-L.; Heux, L. *J. Phys. Chem. B* **2009**, *113*, 11069.
(178) Elazzouzi, S. Ph.D. thesis, Joseph Fourier University, Grenoble, France, 2006.
(179) Revol, J. F.; Godbout, L.; Dong, X. M.; Gray, D. G.; Chanzy, H.; Maret, G. *Liq. Cryst.* **1994**, *16*, 127.
(180) Sugiyama, J.; Chanzy, H.; Maret, G. *Macromolecules* **1992**, *25*, 4232.
(181) Fleming, K.; Gray, D. G.; Prasannan, S.; Matthews, S. *J. Am. Chem. Soc.* **2000**, *122*, 5224.
(182) Kvien, I.; Oksman, K. *Appl. Phys. A: Mater. Sci. Process.* **2007**, *87*, 641.
(183) Habibi, Y.; Heim, T.; Douillard, R. *J. Polym. Sci., Part B: Polym. Phys.* **2008**, *46*, 1430.
(184) Bordel, D.; Putaux, J.-L.; Heux, L. *Langmuir* **2006**, *22*, 4899.
(185) Revol, J. F.; Godbout, L.; Gray, D. G. *J. Pulp Pap. Sci.* **1998**, *24*, 146.
(186) Roman, M.; Gray, D. G. *Langmuir* **2005**, *21*, 5555.
(187) Gray, D. G.; Roman, M. In *Cellulose Nanocomposites: Processing, Characterization, and Properties*; Oksman, K., Sain, M., Eds.; ACS Symposium Series 938; American Chemical Society: Washington, DC, 2006.
(188) Nishiyama, Y.; Langan, P.; Chanzy, H. *J. Am. Chem. Soc.* **2002**, *124*, 9074.
(189) Noorani, S.; Simonsen, J.; Atre, S. In *Cellulose Nanocomposites: Processing, Characterization and Properties*; Oksman, K., Sain, M., Eds.; ACS Symposium Series 938; American Chemical Society: Washington, D.C., 2006.
(190) Morin, A.; Dufresne, A. *Macromolecules* **2002**, *35*, 2190.
(191) Paillet, M.; Dufresne, A. *Macromolecules* **2001**, *34*, 6527.
(192) Azizi Samir, M. A. S.; Alloin, F.; Sanchez, J.-Y.; Dufresne, A. *Polymer* **2004**, *45*, 4149.
(193) Azizi Samir, M. A. S.; Chazeau, L.; Alloin, F.; Cavaille, J. Y.; Dufresne, A.; Sanchez, J. Y. *Electrochim. Acta* **2005**, *50*, 3897.
(194) Azizi Samir, M. A. S.; Mateos, A. M.; Alloin, F.; Sanchez, J.-Y.; Dufresne, A. *Electrochim. Acta* **2004**, *49*, 4667.
(195) Azizi Samir, M. A. S.; Alloin, F.; Sanchez, J.-Y.; Dufresne, A. *Polim.: Cienc. Tecnol.* **2005**, *15*, 109.
(196) Petersson, L.; Mathew, A. P.; Oksman, K. *J. Appl. Polym. Sci.* **2009**, *112*, 2001.
(197) Choi, Y.; Simonsen, J. *J. Nanosci. Nanotechnol.* **2006**, *6*, 633.
(198) Paralikar, S. A.; Simonsen, J.; Lombardi, J. *J. Membr. Sci.* **2008**, *320*, 248.
(199) Chauve, G.; Heux, L.; Arouini, R.; Mazeau, K. *Biomacromolecules* **2005**, *6*, 2025.
(200) Chazeau, L.; Cavaillé, J. Y.; Canova, G.; Dendievel, R.; Boutherin, B. *J. Appl. Polym. Sci.* **1999**, *71*, 1797.
(201) Chazeau, L.; Cavaille, J. Y.; Terech, P. *Polymer* **1999**, *40*, 5333.
(202) Chazeau, L.; Cavaille, J. Y.; Perez, J. *J. Polym. Sci., Part B: Polym. Phys.* **2000**, *38*, 383.
(203) Chazeau, L.; Paillet, M.; Cavaille, J. Y. *J. Polym. Sci., Part B: Polym. Phys.* **1999**, *37*, 2151.
(204) Marcovich, N. E.; Auad, M. L.; Bellesi, N. E.; Nutt, S. R.; Aranguren, M. I. *J. Mater. Res.* **2006**, *21*, 870.
(205) Orts, W. J.; Imam, S. H.; Shey, J.; Glenn, G. M.; Inglesby, M. K.; Guttman, M. E.; Nguyen, A. *Annu. Tech. Conf.-Soc. Plast. Eng.* **2004**, *62*, 2427.
(206) Kvien, I.; Sugiyama, J.; Votrubec, M.; Oksman, K. *J. Mater. Sci.* **2007**, *42*, 8163.
(207) Lu, Y.; Weng, L.; Cao, X. *Macromol. Biosci.* **2005**, *5*, 1101.
(208) Lu, Y.; Weng, L.; Cao, X. *Carbohydr. Polym.* **2006**, *63*, 198.
(209) Wang, Y.; Cao, X.; Zhang, L. *Macromol. Biosci.* **2006**, *6*, 524.
(210) Qi, H.; Cai, J.; Zhang, L.; Kuga, S. *Biomacromolecules* **2009**, *10*, 1597.
(211) Bondeson, D.; Oksman, K. *Composites Part A* **2007**, *38A*, 2486.
(212) Oksman, K.; Mathew, A. P.; Bondeson, D.; Kvien, I. *Compos. Sci. Technol.* **2006**, *66*, 2776.
(213) Petersson, L.; Kvien, I.; Oksman, K. *Compos. Sci. Technol.* **2007**, *67*, 2535.
(214) Dubief, D.; Samain, E.; Dufresne, A. *Macromolecules* **1999**, *32*, 5765.
(215) Dufresne, A. *Compos. Interfaces* **2000**, *7*, 53.
(216) Jiang, L.; Morelius, E.; Zhang, J.; Wolcott, M.; Holbery, J. *J. Compos. Mater.* **2008**, *42*, 2629.
(217) Schroers, M.; Kokil, A.; Weder, C. *J. Appl. Polym. Sci.* **2004**, *93*, 2883.
(218) Azizi Samir, M. A. S.; Alloin, F.; Sanchez, J.-Y.; El Kissi, N.; Dufresne, A. *Macromolecules* **2004**, *37*, 1386.
(219) van den Berg, O.; Schroeter, M.; Capadona, J. R.; Weder, C. *J. Mater. Chem.* **2007**, *17*, 2746.
(220) Viet, D.; Beck-Candanedo, S.; Gray, D. G. *Cellulose* **2007**, *14*, 109.
(221) van den Berg, O.; Capadona, J. R.; Weder, C. *Biomacromolecules* **2007**, *8*, 1353.
(222) Capadona, J. R.; van den Berg, O.; Capadona, L. A.; Schroeter, M.; Rohan, S. J.; Tyler, D. J.; Weder, C. *Nat. Nanotechnol.* **2007**, *2*, 765.
(223) Weder, C.; Capadona, J.; van den Berg, O. (Case Western Reserve University, U., Ed. Application) US 2008/79264, 2008.
(224) Capadona, J. R.; Shanmuganathan, K.; Tyler, D. J.; Rowan, S. J.; Weder, C. *Science* **2008**, *319*, 1370.
(225) Oksman, K.; Bondeson, D.; Syre, P.; (Ntnu Technology Transfer AS, Norway). U.S. Patent Application US 2006/560190, 2008.
(226) Mathew, A. P.; Chakraborty, A.; Oksman, K.; Sain, M. In *Cellulose Nanocomposites: Processing, Characterization, and Properties*; Oksman, K., Sain, M., Eds.; ACS Symposium Series 938; American Chemical Society: Washington, DC, 2006.
(227) Orts, W. J.; Shey, J.; Imam, S. H.; Glenn, G. M.; Guttman, M. E.; Revol, J.-F. *J. Polym. Environ.* **2005**, *13*, 301.
(228) Park, W.-I.; Kang, M.; Kim, H.-S.; Jin, H.-J. *Macromol. Symp.* **2007**, *249/250*, 289.
(229) Medeiros, E. S.; Mattoso, L. H. C.; Ito, E. N.; Gregorski, K. S.; Robertson, G. H.; Offeman, R. D.; Wood, D. F.; Orts, W. J.; Imam, S. H. *J. Biobased Mater. Bioenergy* **2008**, *2*, 1.
(230) Peresin, M. S.; Habibi, Y.; Zoppe, J. O.; Pawlak, J. J.; Rojas, O. J. *Biomacromolecules* **2010**, DOI: 10.1021/bm901254n.
(231) Magalhães, W. L. E.; Cao, X.; Lucia, L. A. *Langmuir* **2009**, *25*, 13250.
(232) Zoppe, J. O.; Peresin, M. S.; Habibi, Y.; Venditti, R. A.; Rojas, O. J. *ACS Appl. Mater. Interfaces* **2009**, *1*, 1996.
(233) Xiang, C.; Joo, Y. L.; Frey, M. W. *J. Biobased Mater. Bioenergy* **2009**, *3*, 147.
(234) Podsiadlo, P.; Choi, S.-Y.; Shim, B.; Lee, J.; Cuddihy, M.; Kotov, N. A. *Biomacromolecules* **2005**, *6*, 2914.
(235) Cranston, E. D.; Gray, D. G. *Biomacromolecules* **2006**, *7*, 2522.

(236) Tashiro, K.; Kobayashi, M. *Polymer* **1991**, *32*, 1516.
(237) Sturcova, A.; Davies, G. R.; Eichhorn, S. J. *Biomacromolecules* **2005**, *6*, 1055.
(238) Rusli, R.; Eichhorn, S. J. *Appl. Phys. Lett.* **2008**, *93*, 033111.
(239) Halpin, J. C.; Kardos, J. L. *J. Appl. Polym.* **1972**, *43*, 2235.
(240) Favier, V.; Canova, G. R.; Shrivastavas, C.; Cavaillé, J. Y. *Polym. Eng. Sci.* **1997**, *37*, 1732.
(241) Flandin, L.; Cavaillé, J. Y.; Bidan, G.; Brechet, Y. *Polym. Compos.* **2000**, *21*, 165.
(242) Stauffer, D.; Aharony, A. *Introduction to Percolation Theory*; Taylor & Francis: London, 1992.
(243) Surve, M.; Pryamitsyn, V.; Ganesan, V. *Phys. Rev. Lett.* **2006**, *96*, 177805.
(244) Garboczi, E. J.; Snyder, K. A.; Douglas, J. F. *Phys. Rev. E: Stat. Phys. Plasmas, Fluids, Relat. Interdiscip. Top.* **1995**, *52*, 819.
(245) Surve, M.; Pryamitsyn, V.; Ganesan, V. *J. Chem. Phys.* **2006**, *125*, 064903.
(246) Prasad, V.; Trappe, V.; Dinsmore, A. D.; Segre, P. N.; Cipellettie, L.; Weitz, D. A. *Faraday Discuss.* **2003**, *123*, 1.
(247) Takayanagi, M.; Uemura, S.; Minami, S. *J. Polym. Sci.* **1964**, *5*, 113.
(248) Ouali, N.; Cavaillé, J.-Y.; Perez, J. *Plast. Rubber Compos. Process. Appl.* **1991**, *16*, 55.
(249) Favier, V.; Dendievel, R.; Canova, G.; Cavaille, J. Y.; Gilormini, P. *Acta Mater.* **1997**, *45*, 1557.
(250) Azizi Samir, M. A. S.; Alloin, F.; Dufresne, A. *Biomacromolecules* **2005**, *6*, 612.
(251) Hajji, P.; Cavaille, J. Y.; Favier, V.; Gauthier, C.; Vigier, G. *Polym. Compos.* **1996**, *17*, 612.
(252) Dufresne, A. *J. Nanosci. Nanotechnol.* **2006**, *6*, 322.
(253) Dufresne, A. *Can. J. Chem.* **2008**, *86*, 484.
(254) Mathew, A. P.; Dufresne, A. *Biomacromolecules* **2002**, *3*, 609.
(255) Azizi Samir, M. A. S.; Alloin, F.; Gorecki, W.; Sanchez, J.-Y.; Dufresne, A. *J. Phys. Chem. B* **2004**, *108*, 10845.
(256) Gray, D. G. *Cellulose* **2008**, *15*, 297.

CR900339W